ACS OMEGA

http://pubs.acs.org/journal/acsodf

Article

Engineering BioBricks for Deoxysugar Biosynthesis and Generation of New Tetracenomycins

Heli Tirkkonen, Katelyn V. Brown, Magdalena Niemczura, Zélie Faudemer, Courtney Brown, Larissa V. Ponomareva, Yosra A. Helmy, Jon S. Thorson, S. Eric Nybo,* Mikko Metsä-Ketelä,* and Khaled A. Shaaban*

Cite This: *ACS Omega* 2023, 8, 21237−21253

Read Online

ACCESS | Metrics & More | Article Recommendations | Supporting Information

ABSTRACT: Tetracenomycins and elloramycins are polyketide natural products produced by several actinomycetes that exhibit antibacterial and anticancer activities. They inhibit ribosomal translation by binding in the polypeptide exit channel of the large ribosomal subunit. The tetracenomycins and elloramycins are typified by a shared oxidatively modified linear decaketide core, yet they are distinguished by the extent of O-methylation and the presence of a 2′,3′,4′-tri-*O*-methyl-α-L-rhamnose appended at the 8-position of elloramycin. The transfer of the TDP-L-rhamnose donor to the 8-demethyl-tetracenomycin C aglycone acceptor is catalyzed by the promiscuous glycosyltransferase ElmGT. ElmGT exhibits remarkable flexibility toward transfer of many TDP-deoxysugar substrates to 8-demethyltetracenomycin C, including TDP-2,6-dideoxysugars, TDP-2,3,6-trideoxysugars, and methyl-branched deoxysugars in both D- and L-configurations. Previously, we developed an improved host, *Streptomyces coelicolor* M1146::cos16F4iE, which is a stable integrant harboring the required genes for 8-demethyltetracenomycin C biosynthesis and expression of ElmGT. In this work, we developed BioBricks gene cassettes for the metabolic engineering of deoxysugar biosynthesis in *Streptomyces* spp. As a proof of concept, we used the BioBricks expression platform to engineer biosynthesis for D-configured TDP-deoxysugars, including known compounds 8-*O*-D-glucosyl-tetracenomycin C, 8-*O*-D-olivosyl-tetracenomycin C, 8-*O*-D-mycarosyl-tetracenomycin C, and 8-*O*-D-digitoxosyl-tetracenomycin C. In addition, we generated four new tetracenomycins including one modified with a ketosugar, 8-*O*-4′-keto-D-digitoxosyl-tetracenomycin C, and three modified with 6-deoxysugars, including 8-*O*-D-fucosyl-tetracenomycin C, 8-*O*-D-allosyl-tetracenomycin C, and 8-*O*-D-quinovosyl-tetracenomycin C. Our work demonstrates the feasibility of BioBricks cloning, with the ability to recycle intermediate constructs, for the rapid assembly of diverse carbohydrate pathways and glycodiversification of a variety of natural products.

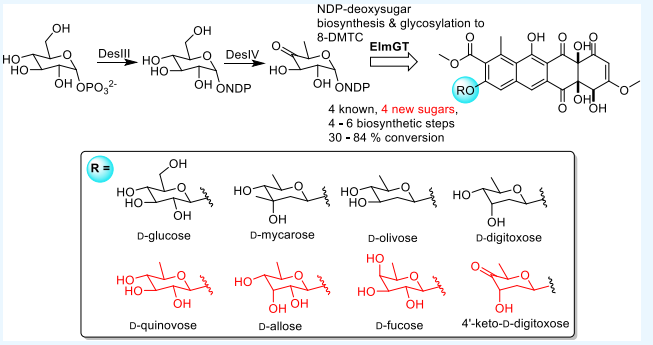

INTRODUCTION

Nature has evolved elaborate enzymatic strategies for both the tailoring of carbohydrate substituents and the attachment of sugar moieties to a parent scaffold.[1] Many natural products feature one or more pendant saccharides as an indispensable feature of their mechanism of action.[2] The pharmacological properties of a natural product pharmacophore can be altered substantially via the pendant carbohydrate moieties, including cellular penetration, potency, efficacy, and clearance, whereas deoxysugars can even contribute hydrophobic and hydrophilic domains for drug−target recognition.[3,4] Furthermore, natural product glycosylation patterns influence the structural diversity of entire families of natural products.[4] A recent comprehensive meta-analysis by Elshahawi et al. revealed that, as of 2015, of the 15,940 bacterial natural products that were described in the literature, 3426 compounds were glycosylated.[5] In addition, Elshahawi et al. revealed that these natural product glycosides were decorated with 344 distinct carbohydrate appendages.[5]

Within the kingdom of prokaryotes, the soil-dwelling actinomycetes have evolved a prolific breadth of biosynthetic enzymes that catalyze the formation of nucleotide-activated deoxysugars and glycosyltransferases that append the sugars to natural product scaffolds.[6] In recent years, biosynthesis of exotic NDP-activated deoxysugars has gained much attention through functional *in vitro* enzyme assays and structural biology of key enzymes.[2] Furthermore, combinatorial biosynthesis has emerged as a mature discipline for *in vivo* engineering of natural product glycosylation patterns. The modification or exchange of carbohydrates to change the structure or function is known as

Received: April 11, 2023
Accepted: May 18, 2023
Published: June 1, 2023

https://doi.org/10.1021/acsomega.3c02460
ACS Omega 2023, 8, 21237−21253

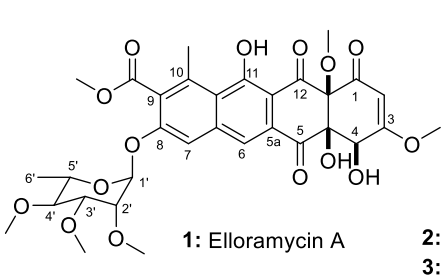

1: Elloramycin A

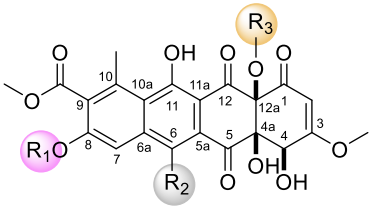

2: R_1=R_2=R_3=H; 8-Demethyltetracenomycin C (8-DMTC)
3: R_1=CH_3, R_2=R_3=H; Tetracenomycin C (TcmC)
4: R_1=R_3=CH_3, R_2=H; Tetracenomycin X (TcmX)
5: R_1=CH_3, R_2=OH, R_3=H; 6-Hydroxy-tetracenomycin C (6-OH-TcmC)
6: R_1=R_3=CH_3, R_2=OH; 6-Hydroxy-tetracenomycin X (6-OH-TcmX)

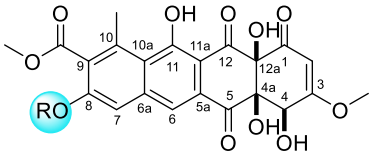

7: R= **I**; 8-Demethyl-8-*O*-*β*-D-glucosyl-tetracenomycin C (DGLU-TCMC)
8: R= **II**; 8-Demethyl-8-*O*-*β*-D-olivosyl-tetracenomycin C (DOLV-TCMC)
9: R= **III**; 8-Demethyl-8-O-*β*-D-digitoxosyl-tetracenomycin C (DDIG-TCMC)
10: R= **IV**; 8-Demethyl-8-*O*-*β*-D-mycarosyl-tetracenomycin C (DMYC-TCMC)
11: R= **V**; 8-Demethyl-8-*O*-(4'-keto)-β-D-digitoxosyl-tetracenomycin C (DKDIG-TCMC)
12: R= **VI**; 8-Demethyl-8-*O*-*β*-D-quinovosyl-tetracenomycin C (DQNV-TCMC)
13: R= **VII**; 8-Demethyl-8-*O*-*β*-D-allosyl-tetracenomycin C (DALO-TCMC)
14: R= **VIII**; 8-Demethyl-8-*O*-*β*-D-fucosyl-tetracenomycin C (DFUC-TCMC)
15: R= **IX**; 8-Demethyl-8-*O*-(2'-methoxyl)-*α*-L-rhamnosyl-tetracenomycin C
16: R= **X**; 8-Demethyl-8-*O*-*β*-D-boivinosyl-tetracenomycin C (DBOV-TCMC)

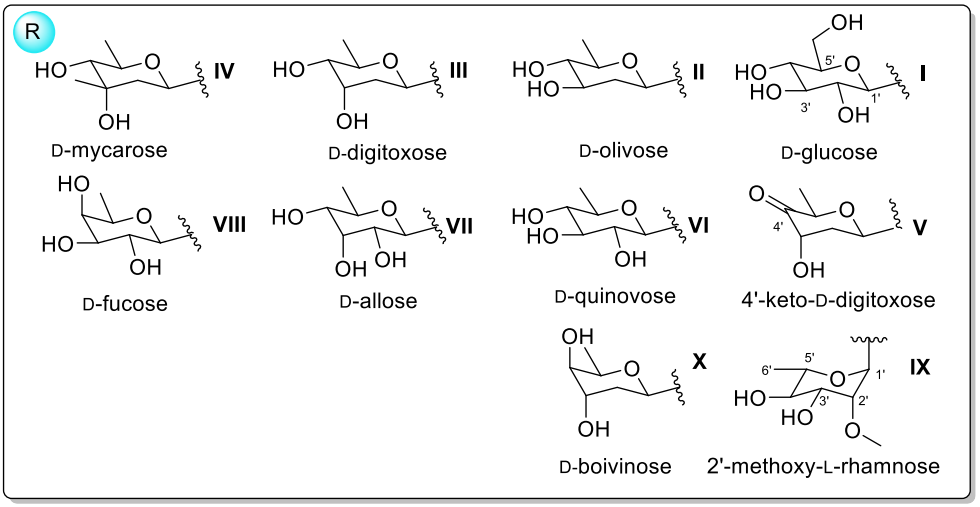

Figure 1. Chemical structures of tetracenomycin natural products discussed in this work.

glycodiversification, and it is a vital strategy for rational drug development.[7]

The elloramycin biosynthetic pathway has been one of the most successful examples with respect to the generation of glycodiversity via combinatorial biosynthesis.[8−12] Elloramycin (**1**) is an aromatic polyketide antibiotic produced by *Streptomyces olivaceus* strain Tü 2353.[13] Elloramycin exhibits antibacterial activity against Gram-positive microorganisms and antiproliferative activity against human cancers via binding to the polypeptide exit channel and inhibition of ribosome translation.[14] Elloramycin features a permethylated 8-*O*-L-rhamnose sugar appendage, which has a poorly understood role in binding of the drug to the large polypeptide exit channel. 8-Demethyl-tetracenomycin C (**2**), tetracenomycins C (**3**) and X (**4**), and 6-hydroxy-tetracenomycins C (**5**) and X (**6**) are additional nonglycosylated congeners previously described from this family[15−19] (Figure 1). The biosynthetic gene cluster (BGC) for elloramycin was previously isolated on cos16F4.[20] Decker et al. demonstrated that heterologous expression of cos16F4 in *Streptomyces lividans* resulted in the production of the aglycone, 8-demethyl-tetracenomycin C (**2**), but not the production of elloramycin due to the absence of genes for the biogenesis of NDP-deoxysugars. Ramos et al. discovered the TDP-L-rhamnose biosynthetic pathway of *S. olivaceus* Tü2353 residues outside of the BGC for the aglycone **2** near genes required for cell wall biosynthesis.[21] The expression of the TDP-L-rhamnose pathway on a second expression vector in trans reconstituted the production of elloramycin.[8,21] Recently, an

https://doi.org/10.1021/acsomega.3c02460
ACS Omega 2023, 8, 21237−21253

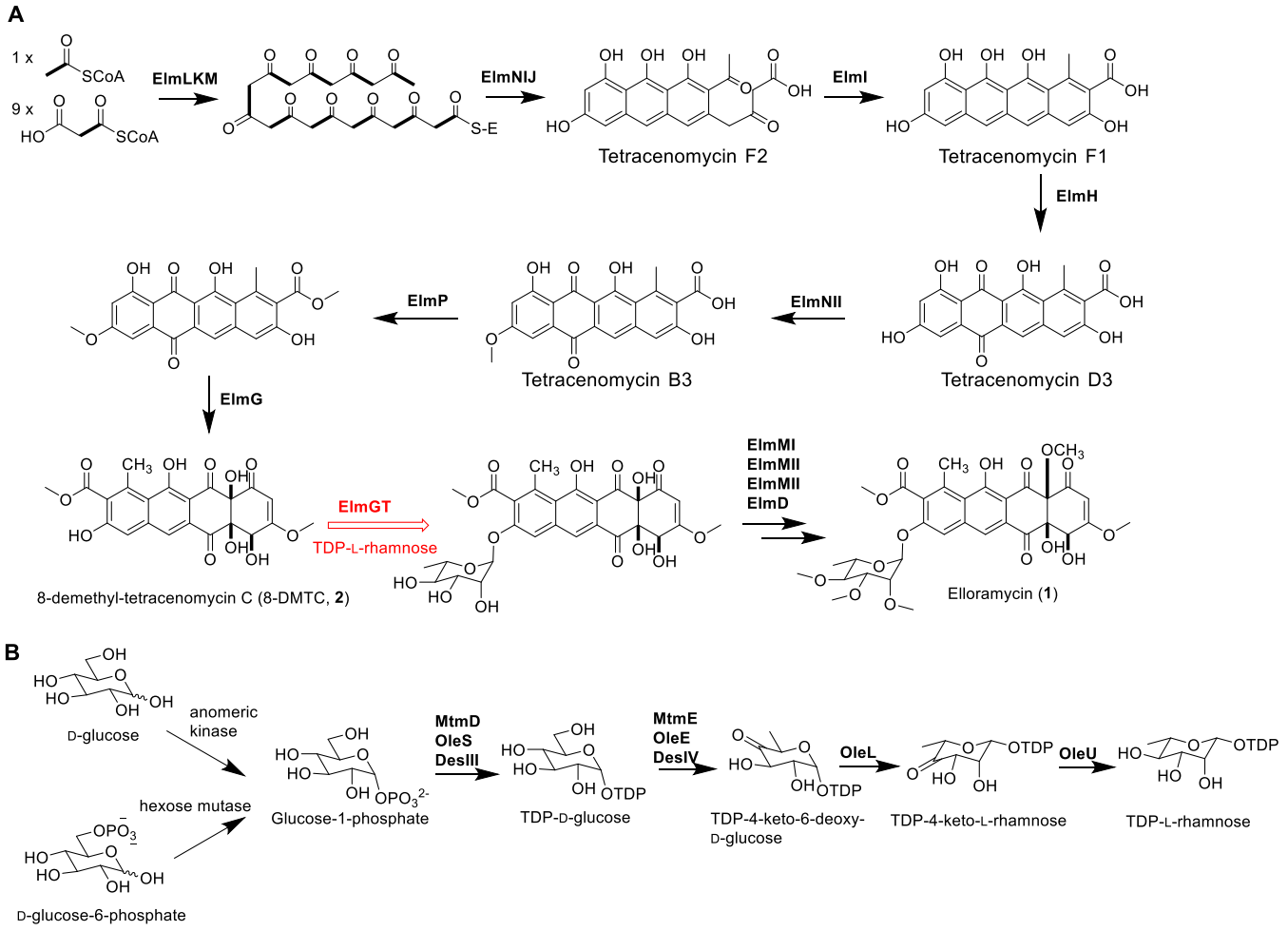

Figure 2. Elloramycin biosynthetic pathway. (A) Elloramycin polyketide synthase pathway. (B) TDP-L-rhamnose deoxysugar biosynthetic pathway.

improved host for the production of **2** was developed via the integration of the *elm* biosynthetic pathway on cos16F4iE into the phiC31 attachment of *Streptomyces coelicolor* M1146 to generate *S. coelicolor*::cos16F4iE.[22]

The *S. coelicolor* M1146::cos16F4iE expression system is an ideal platform for assessing combinatorial biosynthesis of heterologous TDP-deoxysugar pathways due to the presence of the "sugar donor flexible" glycosyltransferase ElmGT. The elloramycin glycosyltransferase exhibits relaxed substrate specificity toward many TDP-deoxysugar substrates, including TDP-2,6-dideoxysugars, TDP-2,3,6-trideoxysugars, and branched-chain deoxysugars in both D- and L-configurations. This relaxed substrate specificity has resulted in the production of >20 glycosylated derivatives of **2**.[8−12,23−25] However, the antiproliferative activity of many of these analogues and the role of the carbohydrate in fostering binding to the ribosomal polypeptide exit channel are largely unknown.

In this work, we developed a BioBricks synthetic biology system for cloning TDP-deoxysugar operons in "sugar plasmids" that were expressed in *S. coelicolor* M1146::cos16F4iE. As a proof of concept, four known tetracenomycins with D-configured deoxysugars were biosynthesized in the actinomycete system, including 8-demethyl-8-*O*-*β*-D-glucosyl-tetracenomycin C (**7**), 8-demethyl-8-*O*-*β*-D-olivosyl-tetracenomycin C (**8**), 8-demethyl-8-*O*-*β*-D-digitoxosyl-tetracenomycin C (**9**), and 8-demethyl-8-*O*-*β*-D-mycarosyl-tetracenomycin C (**10**). In addition, we biosynthesized four new tetracenomycins, including 8-demethyl-8-*O*-(4′-keto)-*β*-D-digitoxosyl-tetracenomycin C (**11**), 8-demethyl-8-*O*-*β*-D-quinovosyl-tetracenomycin C (**12**), 8-demethyl-8-*O*-*β*-D-allosyl-tetracenomycin C (**13**), and 8-demethyl-8-*O*-*β*-D-fucosyl-tetracenomycin C (**14**). These compounds were assessed for their antiproliferative activity in human cancer cell lines and antibacterial activity against a panel of Gram-positive and Gram-negative bacteria along with **1**−**3** and 8-demethyl-8-*O*-(2′-methoxy)-*α*-L-rhamnosyl-TCMC (**15**)[26] from the Center for Pharmaceutical Research and Innovation (CPRI) repository. In total, this work demonstrates the utility of the elloramycin BioBricks synthetic biology system for investigating new deoxysugar metabolism.

RESULTS AND DISCUSSION

BioBricks Cloning of the TDP-L-rhamnose Pathway for Elloramycin Production. Elloramycin biosynthesis is initiated by the ElmKLM aromatic polyketide synthase (PKS), which condenses 1× acetyl-CoA starter units and 9× malonyl-CoA extender units to form the decaketide poly-*β*-ketothioester (Figure 2A). This intermediate is cyclized by ElmNIJ, oxidized by ElmH, methylated by ElmNII and ElmP, before undergoing triple hydroxylation by ElmG to yield **2**.[19,27−29] The glycosyltransferase ElmGT transfers TDP-L-rhamnose to the 8-OH of **2** to form 8-demethyl-8-*O*-*α*-L-rhamnosyl-tetracenomycin C, which undergoes methylations at the 2′, 3′, 4′, and 12a-positions to generate **1** (Figure 2A).

https://doi.org/10.1021/acsomega.3c02460
ACS Omega 2023, 8, 21237−21253

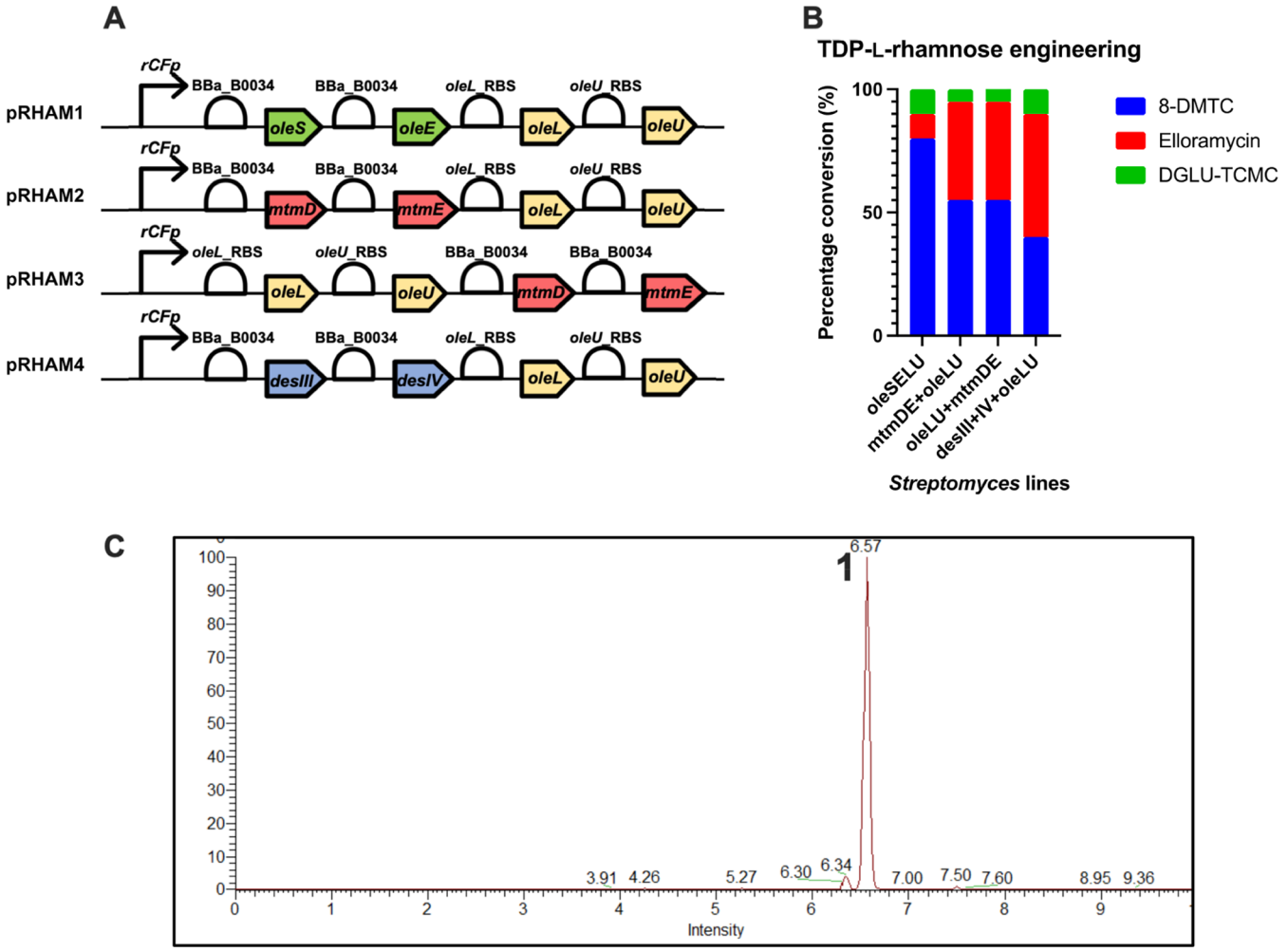

Figure 3. (A) SBOL vector diagrams for TDP-L-rhamnose sugar plasmids. (B) Engineering of *S. coelicolor* M1146::cos16F4iE for the production of **1**. Constructs pRHAM1 (oleSELU), pRHAM2 (mtmDE + oleLU), pRHAM3 (oleLU + mtmDE), and pRHAM4 (desIII + desIV + oleLU) were independently transformed, and six biological replicates were picked per comparison. The percentage conversion (%) of **2** to **1** was measured for each strain by integrating peak areas in the high-performance liquid chromatography (HPLC)−ultraviolet−visible (UV−vis) traces at 412 nm. (C) Representative extracted ion chromatogram of elloramycin (**1**) from cell extracts of *S. coelicolor* M1146::cos16F4iE/pRHAM3 [m/z = 661.2109 $[M + H]^+$]. Data were acquired by Michigan State University, Mass Spectrometry and Metabolomics Core on a Thermo Q-exactive UPLC-MS/MS.

Antibiotic deoxysugar biosynthetic pathways are initiated with the activation of D-glucose and progression through consecutive deoxygenation reactions (Figure 2B).[30] The sugar donor, TDP-L-rhamnose, is generated from D-glucose in five enzymatic steps (Figure 2B). D-Glucose is phosphorylated by anomeric kinase, or D-glucose-6-phosphate is interconverted to D-glucose-1-phosphate. TDP-D-glucose synthase (e.g., MtmD, OleS, DesIII) transfers thymidine monophosphate to D-glucose-1-phosphate to form TDP-D-glucose. TDP-D-glucose-4,6-dehydratase (MtmE, OleE, DesIV) catalyzes 6-deoxygenation to form the key intermediate TDP-4-keto-6-deoxy-D-glucose. OleL catalyzes epimerization at the 3- and the 5-positions to convert TDP-4-keto-6-deoxy-D-glucose from a $^4C_1$ configuration to a $^1C_4$ configuration. Finally, OleU reduces the 4-ketone to yield TDP-L-rhamnose.

To test the efficiency of *S. coelicolor* M1146::cos16F4iE as an *in vivo* chassis for the production of elloramycin, we designed four BioBricks gene cassettes encoding the TDP-L-rhamnose biosynthetic pathways, pRHAM1, pRHAM2, pRHAM3, and pRHAM4 (Figure 3A). Since TDP-D-glucose synthase and TDP-D-glucose-4,6-dehydratase are the dedicated steps for the biosynthesis of deoxysugar intermediates and several different orthologs for these steps have been described in the literature,[8,25,31−34] we cloned alternative versions of the metabolic pathway to identify the best performing construct (Table 1). The *mtmDE* genes from the mithramycin biosynthetic pathway, *oleSE* genes from the oleandomycin pathway, and the *desIII-IV* genes from the pikromycin biosynthetic pathway were all cloned as BioBricks with the strong BBa_B0034 ribosome entry site into pSB1C3-J04450.[35−37] The genes were spliced under the control of the strong *rCFp* promoter and cloned into the *Streptomyces*−*Escherichia coli* multicopy shuttle vector pUWL201PWBB.[38,39] Genes *oleL* and *oleU* were cloned from the plasmid pLN2 as BioBricks fragments and cloned into the pCR-Blunt II-TOPO vector and sequenced.[8] The construct pRHAM1 encoded the *oleSELU* genes, pRHAM2 encoded the *mtmDE* + *oleLU* genes, pRHAM3 encoded *oleLU* + *mtmDE* in an alternative operonic arrangement, and pRHAM4 encoded *desIII-IV* + *oleLU* (Table 1 and Figure 3A). Expression of all four constructs in *S. coelicolor* M1146::cos16F4iE resulted in the detectable production of **1** with differing efficiencies (Figure 3B). The production of **1** was confirmed based on high-resolution mass spectrometry measurements [(+)-HRESI-MS: m/z 661.2109 $[M + H]^+$

https://doi.org/10.1021/acsomega.3c02460
ACS Omega 2023, 8, 21237−21253

Table 1. List of Plasmids Constructed and/or Used in This Study

plasmid	genotype and relevant characteristics	reference
pUWL201PWBB	*bla*^{R}, *tsr*^{R}, *fd* terminator, pIJ101 *ori*, ColE1 *ori*, MCS, *oriT*, MCS	this study
pRHAM1	*oleSELU* (TDP-L-rhamnose) operon under control of *rCFp*	this study
pRHAM2	*mtmDE* + *oleLU* (TDP-L-rhamnose) operon under control of *rCFp*	this study
pRHAM3	*oleLU* + *mtmDE* (TDP-L-rhamnose) operon under control of *rCFp*	this study
pRHAM4	*desIII* + *desIV* + *oleLU* (TDP-L-rhamnose) operon under control of *rCFp*	this study
pDOLV	*desIII* + *desIV* + *oleVW* + *urdR* (TDP-D-olivose) operon under control of *rCFp*	this study
pDDIG	*desIII* + *desIV* + *oleV* + *eryBII* + *urdR* (TDP-D-digitoxose) operon under control of *rCFp*	this study
pDMYC	*desIII* + *desIV* + *oleVW* + *cmmC* + *mtmTIII* (TDP-D-mycarose) operon under control of *rCFp*	this study
pDBOV	*desIII* + *desIV* + *oleVWU* (TDP-D-boivinose) operon under control of *rCFp*	this study
pDBOV*	*desIII* + *desIV* + *oleVWU** (TDP-D-boivinose) operon under control of *rCFp*, with repaired version of *oleU*	this study
pDALO	*desIII* + *desIV* + *gerF* + *gerK1* (TDP-D-allose) operon under control of *rCFp*	this study
pDFUCO	*desIII* + *desIV* + *gilU* + *gilV* (TDP-D-fucose) operon under control of *rCFp*	this study
pDARO	*desIII* + *desIV* + *rubS3* (TDP-D-antiarose) operon under control of *rCFp*	this study

(calcd for $C_{32}H_{37}O_{15}$ [M + H]$^+$, 661.2127)] (Figure 3C). During these studies, we detected the production of another tetracenomycin analogue with a parental mass ion in ESI-MS +ve mode (m/z = 621 [M + H]$^+$), which corresponded to the attachment of D-glucose (Figure S24). The compound 8-demethyl-8-*O*-D-glucosyl-tetracenomycin C (**7**) was previously shown to result from the attachment of TDP-D-glucose (e.g., which is an intermediate in all antibiotic deoxysugar biosynthetic pathways, Figure 4) to **2**.[23] This result could be explained by the inefficiency of some of the L-rhamnose biosynthetic pathways encoded by the constructs above, resulting in the production of **7** due to the relaxed substrate preference of ElmGT (Table 2).

Compounds **1**, **2**, and **7** were extracted and purified by various chromatographic methods. The physicochemical properties of compounds **1**, **2**, and **7** are summarized in the Materials and Methods section. Compounds **1**, **2**, and **7** were obtained as yellow solids with UV/vis characteristics typical to tetracenomycins. The chemical structures of compounds **1**, **2**, and **7** were established by MS and 1D (^{1}H and ^{13}C NMR) and 2D (heteronuclear single quantum coherence (HSQC), ^{1}H,^{1}H-correlated spectroscopy (^{1}H,^{1}H-COSY), heteronuclear multiple bond correlation (HMBC), and nuclear Overhauser effect spectroscopy (NOESY)) NMR data analysis (Figures 5, 6, and S5−S33 and Tables S1−S4) and by comparison with standard and literature data. The attachments of the sugar residues at the 8-position in compounds **1** and **7** have been established based on the critical HMBC correlation from H-1′ to C-8. All of the

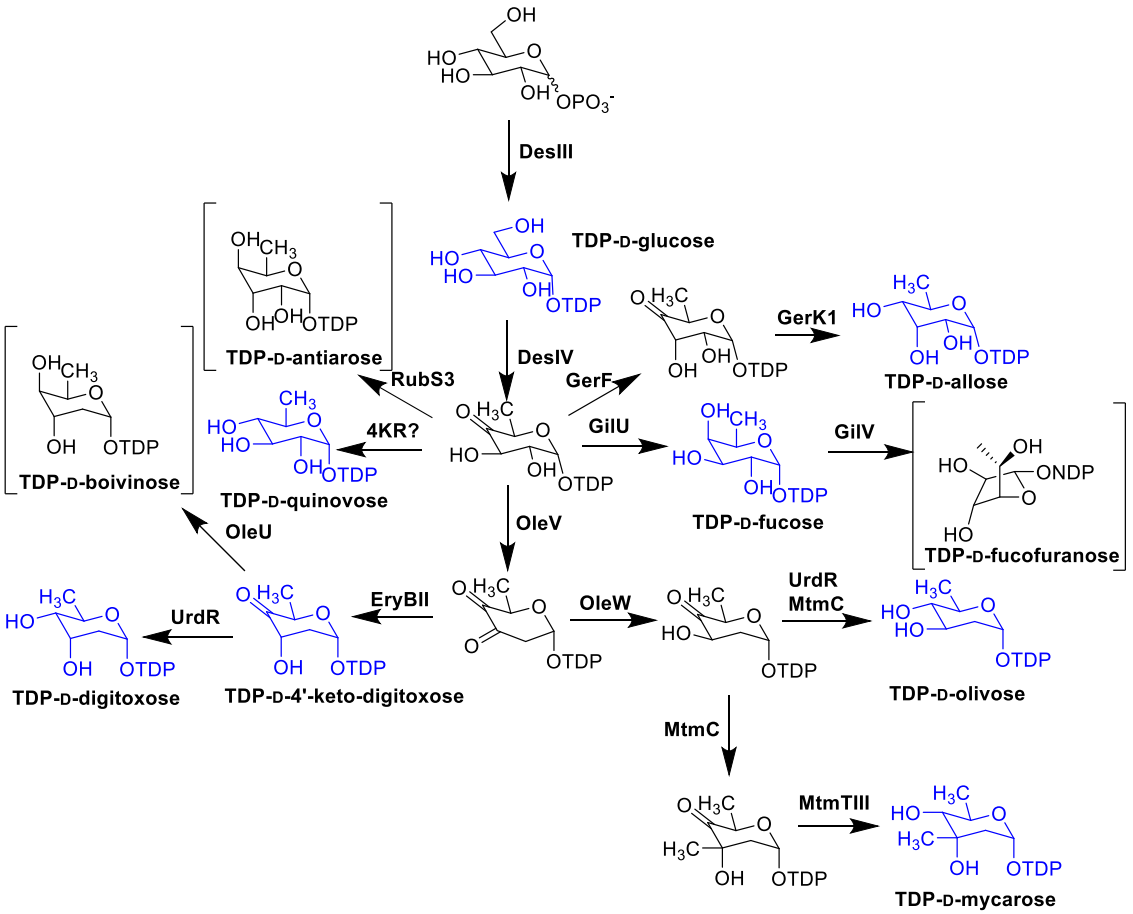

Figure 4. Deoxysugar nucleotide pathways engineered in this work. Sugars in blue were successfully transferred to **2** by ElmGT. Sugars in brackets were the intended biosynthetic end products but were either not formed and/or transferred to **2** by ElmGT.

https://doi.org/10.1021/acsomega.3c02460
ACS Omega 2023, 8, 21237−21253

Table 2. Bacterial Strains Used in This Study

strain	genotype or comments	source or reference
E. coli JM109	*F′ traD36 proA + B+ lacIq Δ(lacZ)M15/Δ(lac-proAB) glnV44 e14-gyrA96 recA1 relA1 endA1 thi hsdR17*	Promega
E. coli ET12567/(pUZ8002)	*dam-dcm-hsdM hsdS hsdR cat tet*; carrying plasmid pUZ8002	40
S. coelicolor M1146	SCP1-SCP2-Δ*act* Δ*red* Δ*cpk* Δ*cda*	41
S. coelicolor M1146::cos16F4iE	SCP1-SCP2-Δ*act* Δ*red* Δ*cpk* Δ*cda*, cos16F4iE integrated into *ϕ*C31 *attB* chromosomal locus	22
S. coelicolor M1146::cos16F4iE/pUWL	*S. coelicolor* M1146::cos16F4iE transformed with plasmid pUWL201PWBB	this study
S. coelicolor M1146::cos16F4iE/pRHAM1	*S. coelicolor* M1146::cos16F4iE transformed with plasmid pRHAM1	this study
S. coelicolor M1146::cos16F4iE/pRHAM2	*S. coelicolor* M1146::cos16F4iE transformed with plasmid pRHAM2	this study
S. coelicolor M1146::cos16F4iE/pRHAM3	*S. coelicolor* M1146::cos16F4iE transformed with plasmid pRHAM3	this study
S. coelicolor M1146::cos16F4iE/pRHAM4	*S. coelicolor* M1146::cos16F4iE transformed with plasmid pRHAM4	this study
S. coelicolor M1146::cos16F4iE/pDOLV	*S. coelicolor* M1146::cos16F4iE transformed with plasmid pDOLV	this study
S. coelicolor M1146::cos16F4iE/pDDIG	*S. coelicolor* M1146::cos16F4iE transformed with plasmid pDDIG	this study
S. coelicolor M1146::cos16F4iE/pDMYC	*S. coelicolor* M1146::cos16F4iE transformed with plasmid pDMYC	this study
S. coelicolor M1146::cos16F4iE/pDBOV	*S. coelicolor* M1146::cos16F4iE transformed with plasmid pDBOV	this study
S. coelicolor M1146::cos16F4iE/pDBOV*	*S. coelicolor* M1146::cos16F4iE transformed with plasmid pDBOV*	this study
S. coelicolor M1146::cos16F4iE/pDALO	*S. coelicolor* M1146::cos16F4iE transformed with plasmid pDALO	this study
S. coelicolor M1146::cos16F4iE/pDFUCO	*S. coelicolor* M1146::cos16F4iE transformed with plasmid pDFUCO	this study
S. coelicolor M1146::cos16F4iE/pDARO	*S. coelicolor* M1146::cos16F4iE transformed with plasmid pDARO	this study

remaining 2D NMR (^{1}H,^{1}H-COSY, HMBC, and NOESY) correlations are in full agreement with structures **1**, **2**, and **7** (Figure 6 and Tables S1−S4).

The best performing construct was pRHAM4, which converted approximately 60% of **2** to **1**, whereas pRHAM2 and pRHAM3 converted approximately 40−45% of **2** to **1**, and pRHAM1 converted approximately 10% of **2** to **1** (Figure 3B). These experiments demonstrated that the TDP-D-glucose synthase and TDP-D-glucose-4,6-dehydratase enzymes exhibited different catalytic efficiencies *in vivo*, with the *desIII*−*desIV* gene products being the most competent in heterologous expression trials. Interestingly, there was no significant difference in performance between pRHAM2 and pRHAM3 in terms of **1** production, which indicated that operonic arrangement did not significantly alter *in vivo* biosynthesis of TDP-L-rhamnose. Based on these results, we used pRHAM4 as a template for the construction of other sugar pathways.

Heterologous Expression and Structure Elucidation of Tetracenomycins Engineered with 2,6-Dideoxysugar Pathways. To generate a library of analogues for structure−activity studies, we focused on engineering the production of 2,6-dideoxysugars. The various sugar plasmids were cloned as BioBricks gene cassettes in the multicopy expression vector pUWL201PWBB (Table 1).[39] The sugar nucleotide pathways starting from TDP-4-keto-6-deoxy-D-glucose branch off in different directions via additional deoxygenations, transaminations, methylations, and ketoreduction to afford a wide range of TDP-deoxysugars (Figure 4). The biosynthetic pathways for TDP-D-olivose, TDP-D-digitoxose, and TDP-D-boivinose were previously characterized by Pérez and co-workers.[10] In brief, TDP-4-keto-6-deoxy-D-glucose undergoes 2,3-dehydration (OleV) and 3-ketoreduction (OleW), followed by 4-ketoreduction by UrdR to generate TDP-D-olivose (Figure 4). To further illustrate the combinatorial biosynthetic approach toward generating diverse sugar nucleotides, the exchange of the 3-ketoreductase gene *oleW* with the 3-ketoreductase from the erythromycin pathway, *eryBII*, results in an axial-configured 3′-OH (Figure 4). The resulting intermediate can be intercepted by UrdR to yield TDP-D-digitoxose or OleU to provide TDP-D-boivinose (Figure 4).[10]

The expression of the TDP-D-olivose cassette resulted in the conversion of approximately 84% of all tetracenomycins to 8-demethyl-8-*O*-*β*-D-olivosyl-tetracenomycin C (**8**) (Figure 5A−C). In addition, engineering of the TDP-D-digitoxose cassette resulted in the conversion of approximately 60−65% of all tetracenomycins to produce 8-demethyl-8-*O*-*β*-D-digitoxosyl-tetracenomycin C (**9**) (Figure 5D).[10] The compounds **8** and **9** were both detected via their parental mass ions in ESI-MS −ve mode (m/z = 587 $[M - H]^-$), corresponding to the attachment of a 2,6-dideoxysugar to **2**. Compounds **8** and **9** were established to have the same molecular formula ($C_{28}H_{28}O_{14}$) on the basis of high-resolution mass spectrometry (HRMS) data. The NMR data of both isomers **8** and **9** indicated that differences were mainly in the sugar residues attached at the 8-position (Tables S1−S4). The stereochemistry of the sugar residues in compounds **8** and **9** were established based on the coupling constants and/or NOESY correlations and by comparison with literature data. More specifically, the coupling constants of H-4′ (δ_H 3.01, t, J = 8.9 Hz) in compound **8** was different from coupling constants of H-4′ (δ_H 3.34, ddd, J = 2.7, 5.0, 9.0 Hz) in compound **9**. This established the axial orientation of the protons at the 3′-, 4′-, 5′-positions of the sugar residue of compound **8**. However, in compound **9**, the proton at the 3′-position was equatorially oriented, which has been further established by NOESY correlations. All of the remaining 1D and 2D NMR (^{1}H,^{1}H-COSY, HMBC, and NOESY) correlations are in full agreement with structures **8** and **9** as depicted in Figures 1 and 6 (Tables S1−S4 and Figures S34−S46).

We next decided to engineer the TDP-D-mycarose biosynthetic pathway to demonstrate the production of branched sugars.[42,43] TDP-D-olivose and TDP-D-mycarose are sugars found in the mithramycin biosynthetic pathway, and their biosynthesis features a unique bifunctional 4-ketoreductase and 3-*C*-methyltransferase enzyme, MtmC.[44] The activity of MtmC

https://doi.org/10.1021/acsomega.3c02460
ACS Omega 2023, 8, 21237−21253

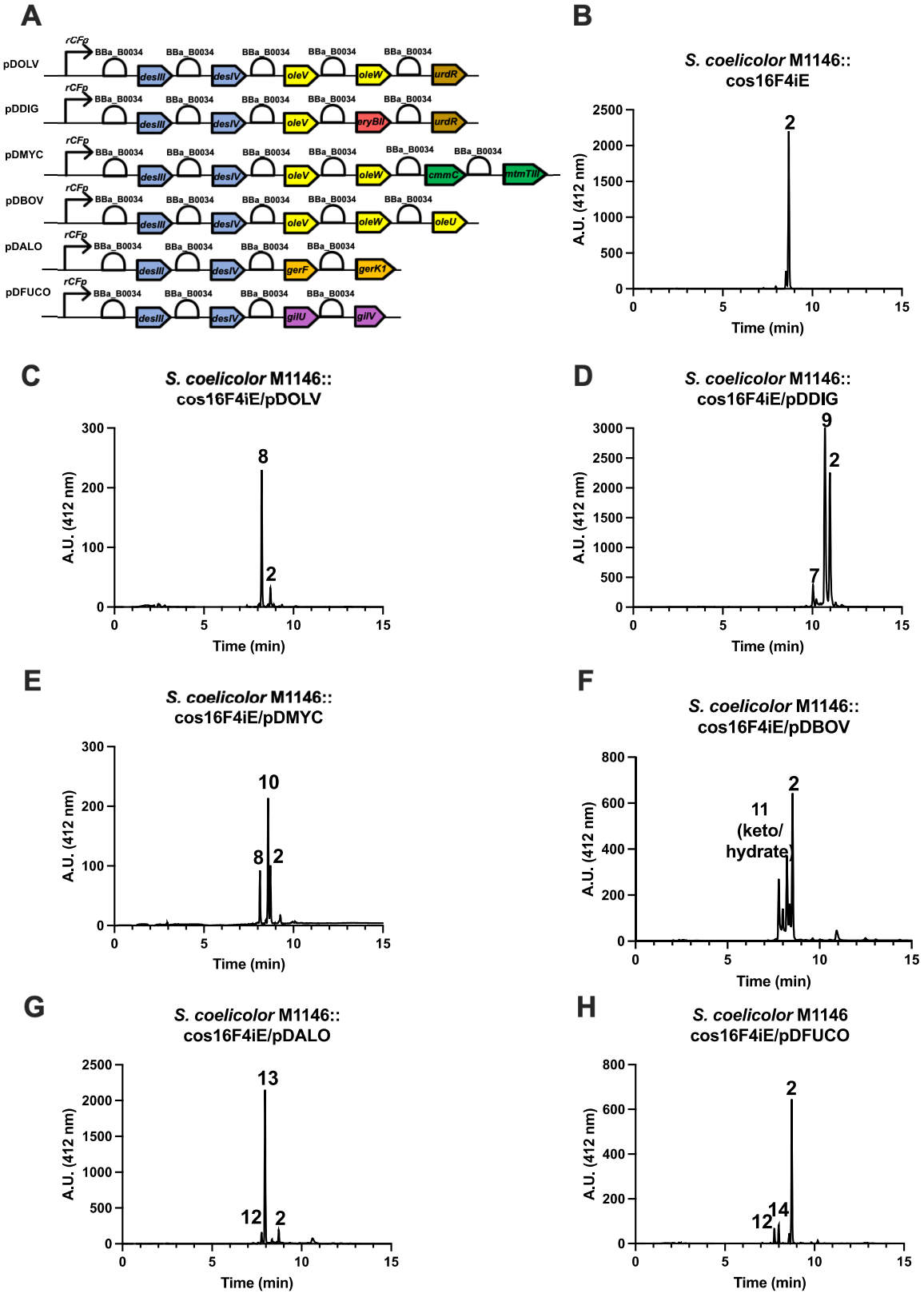

Figure 5. (A) SBOL diagrams of TDP-2,6-dideoxysugar and TDP-6-deoxysugar gene cassettes. Genes are color-coded corresponding to the originating biosynthetic gene cluster (blue = *Streptomyces venezuelae* ATCC15439, pikromycin; yellow = *Streptomyces antibioticus* ATCC 11891, oleandomycin; brown = *Streptomyces fradiae* Tü 2717, urdamycin; green = *Streptomyces griseus* subsp. griseus ATCC 13273 and *Streptomyces argillaceus* ATCC 12956, aureolic acids chromomycin A3, and mithramycin; orange = *Streptomyces* sp. KCTC 0041BP, dihydrochalcomycin; purple = *Streptomyces griseoflavus* Gö 3592). (B–F) HPLC–UV–vis chromatograms of production spectra of cell extracts from *S. coelicolor* M1146::cos16F4iE harboring the different gene cassettes. (B) *S. coelicolor* M1146::cos16F4iE (no plasmid) (C) pDOLV, (D) pDDIG, (E) pDMYC, (F) pDBOV, (G) pDALO, and (H) pDFUCO.

https://doi.org/10.1021/acsomega.3c02460
ACS Omega 2023, 8, 21237–21253

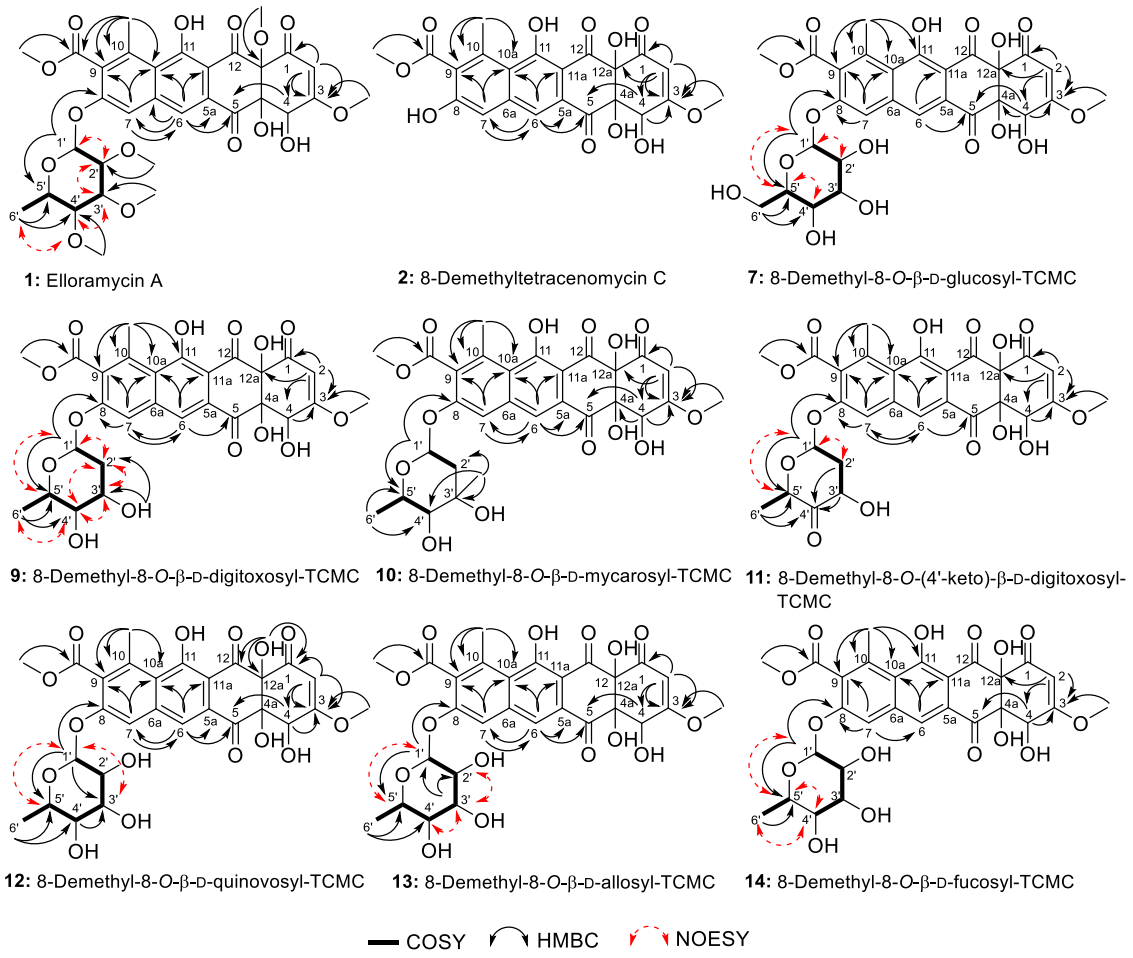

Figure 6. ^{1}H,^{1}H-COSY (—), selected HMBC (→), and selected NOESY (⇢) correlations of compounds **1**, **2**, **7**, and **9**–**14**.

is dictated by the binding of cofactors: binding of NADPH results in the 4-ketoreduction of TDP-4-keto-2,6-dideoxy-D-glucose to generate TDP-D-olivose, whereas the binding of *S*-adenosyl-methionine (SAM) results in 3-*C*-methylation of the same sugar to afford TDP-4-keto-3-*C*-methyl-2,6,-dideoxy-D-glucose.[45] MtmTIII then reduces the ketosugar to TDP-D-mycarose (Figure 4).[43]

Previously, ElmGT was demonstrated to turn over TDP-D-mycarose when cos16F4 was heterologously expressed in the mithramycin producer *S. argillaceus*.[46] We decided to clone a gene cassette encoding the full TDP-D-mycarose pathway for combinatorial biosynthesis of this unique branched sugar. In this study, we decided to assess the uncharacterized *cmmC* *C*-methyltransferase from the related chromomycin A3 pathway.[47] Since the chromomycin A3 pathway encodes a separate 4-ketoreductase implicated in the formation of TDP-D-olivose (e.g., *cmmUII*),[48] we hypothesized that *cmmC* might function as a true *C*-methyltransferase without the additional 4-ketoreductase function. We generated a cassette encoding *desIII* + *desIV* + *oleV* + *oleW* + *cmmC* + *mtmTIII* and transformed the construct into *S. coelicolor* M1146::cos16F4iE (Table 1).

As expected, the strain produced 80% of all tetracenomycins as 8-demethyl-8-*O*-*β*-D-mycarosyl-tetracenomycin C (**10**), as determined based on the m/z = 603 $[M + H]^+$ peak in the ESI-MS +ve mode spectrum (Figure 5E). Surprisingly, **8** was also produced, composing 20% of all tetracenomycins in the extract. The ^{1}H and ^{13}C NMR data of compound **10** were very similar to compound **9**, with the exception of an extra methyl group (δ_H 1.32 (s); δ_C 27.2). The attachment of the methyl group was confirmed at the 3′-position based on the HMBC correlation from 3′-CH_3 (δ_H 1.32) to C-2′/C-3′/C-4′. Cumulative analyses of 1D (^{1}H, ^{13}C) and 2D (HSQC, ^{1}H,^{1}H-COSY, and HMBC) (Figures 6 and S47–S54 and Tables S1 and S3) and the comparison with literature data established the structure of **10** as 8-demethyl-8-*O*-*β*-D-mycarosyl-tetracenomycin C. This result demonstrated that *cmmC* likely encodes a similar bifunctional 4-ketoreductase and 3-*C*-methyltransferase enzyme like *mtmC*, which could explain the production of both **8** and **10** in the same strain.

We then exchanged the *urdR* 4-ketoreductase from the TDP-D-olivose cassette to the *oleU* 4-ketoreductase to render TDP-D-boivinose (Table 1).[48] Engineering of the TDP-D-boivinose pathway resulted in the unexpected production of a new glycosylated tetracenomycin, 8-demethyl-8-*O*-(4′-keto)-*β*-D-digitoxosyl-tetracenomycin C (**11**), which was apparently modified with a ketosugar. The new compound exhibited a parental mass of m/z = 585 $[M - H]^-$ peak corresponding to both a ketosugar and an m/z = 603 $[M + H_2O]^-$ peak corresponding to a hydrate in the negative mode ESI-MS spectrum (Figure 5F). Compound **11** was purified by semi-preparative HPLC and subjected for HRMS and NMR structure elucidation. The molecular formula of **11** was deduced as $C_{28}H_{26}O_{14}$ on the basis of (−)-HRESI-MS [m/z = 585.1250 $[M - H]^-$ (calcd for $C_{28}H_{25}O_{14}$, 585.1250)] and (+)-HRESI-MS [m/z = 587.1385 $[M + H]^+$ (calcd for $C_{28}H_{27}O_{14}$, 587.1395)] and NMR data. The molecular weight and molecular formula

https://doi.org/10.1021/acsomega.3c02460
ACS Omega 2023, 8, 21237−21253

differences between **11** and **9**, established compound **11** to have two protons less than **9**, which may be due to the presence of a ketonic group in **11** instead of a free hydroxyl group in **9**. By comparison of the ^{1}H and ^{13}C NMR data of **9** and **11** (Tables S2 and S4), the H-4′ (δ_H 3.34, ddd, J = 2.7, 5.0, 9.0 Hz; δ_C 73.4) in compound **9** was absent in compound **11** and replaced by a nonprotonated carbon at δ_C 94.1 (C-4′). The chemical shift of the C-4′ (δ_C 94.1) of compound **11** indicates the presence of this carbon atom in its hydrate form in solution. Cumulative analyses of 1D (^{1}H, ^{13}C) and 2D (HSQC, ^{1}H,^{1}H-COSY, HMBC, and NOESY) (Figures 6 and S55−S64 and Tables S2 and S4) established the structure of **11** as depicted in Figure 1. Thus, **11** was established as new natural product, closely related to compound **9** and named as 8-demethyl-8-*O*-(4′-keto)-*β*-D-digitoxosyl-tetracenomycin C.

This was a surprising result since ElmGT had been previously shown to accept the TDP-D-boivinose sugar with a good conversion efficiency to 8-demethyl-8-*O*-*β*-D-boivinosyl-tetracenomycin C.[10] The result suggested that TDP-4′-keto-D-digitoxose was serendipitously transferred to the **2** aglycone. ElmGT was previously demonstrated to transfer TDP-4′-keto-L-olivose to **2**, making this only the second such tetracenomycin analogue modified with a 4′-ketosugar.[12] The result could be explained by a sequencing discrepancy in the originally deposited sequence by Salas and co-workers in the *oleU* 4-ketoreductase gene. Upon resequencing of the original pLN2 plasmid, discrepancies were discovered in the *oleL* 3,5-epimerase gene and the *oleU* 4-ketoreductase gene, which indicated that *oleU* might not be functioning correctly in the construct (Schema S1). As a result, all other constructs using the *oleU* and *oleL* genes were sequenced and the cassettes were resynthesized to match the corrected nucleotide sequences. Repairing the sequence mutations TDP-D-boivinose construct (e.g., pDBOV) resulted in the production of the expected 8-demethyl-8-*O*-*β*-D-boivinosyl-tetracenomycin C (**16**) when the repaired construct was expressed *in vivo* (Figure S102).

Heterologous Expression and Structure Elucidation of Tetracenomycins Engineered with 6-Deoxysugar Pathways. Following the successful reconstitution of 2,6-dideoxysugar pathways in M1146::cos16F4iE, we next turned our attention to the engineering of D-configured 6-deoxysugars. Since TDP-L-rhamnose is the native donor substrate for ElmGT, we hypothesized that ElmGT should also be able to catalyze the transfer of other 6-deoxysugars. The generated compounds would increase the chemical diversity of the tetracenomycins and provide valuable insights into the structure−activity relationship of the sugar moiety and the antiproliferative and antibacterial activities of these compounds.

We turned our sights to TDP-D-allose from the dihydrochalcomycin pathway. TDP-D-allose is metabolized from TDP-4-keto-6-deoxy-D-glucose via the actions of epimerase GerF and 4-ketoreductase GerK1.[49,50] We cloned the TDP-D-allose cassette (e.g., *desIII* + *desIV* + *gerF* + *gerK1*) and expressed it in *S. coelicolor* M1146::cos16F4iE (Table 1). The resulting strains produced two new tetracenomycins, which exhibited parent mass ions of m/z = 603 $[M - H]^-$, indicating the successful attachment of two different 6-deoxysugars (Figure 5G). To establish the chemical structures of compounds **12** and **13**, both compounds were purified and subjected for full spectrometric and spectroscopic data analyses. Like those of **8** and **9**, compounds **12** and **13** were established to have an identical molecular weight (m/z = 604 Da) and molecular formula ($C_{28}H_{28}O_{15}$) on the basis of (−)- and (+)-HRMS and NMR data. By comparison of the ^{1}H and ^{13}C NMR data of both compounds **12** and **13** (Tables S1 and S3), they were identical except for minor changes in the shift/coupling constants of the sugar residues. Specifically, the coupling constant of H-4′ (δ_H 2.92, t, J = 8.6 Hz) in compound **12** confirms that this proton should be an axial/axial coupled with H-3′ and H-5′. However, the coupling constant of H-4′ (δ_H 3.15, dd, J = 9.5, 2.8 Hz) in compound **13** confirms that this proton as an axial/axial (H-4′/H-5′) and axial/equatorial (H-4′/H-3′) coupled. This also was further supported by the small coupling constant of H-3′ (δ_H 3.90, t, J = 2.9 Hz), confirming its equatorial/axial coupling with both H-2′ and H-4′. The stereochemistry of the sugar residues in compounds **12** and **13** was further established based on NOESY correlations and by comparison with literature data. This established that both compounds **12** and **13** were different solely at the stereochemistry of the 3′-position of the sugar residues. Cumulative analyses of 1D (^{1}H, ^{13}C) and 2D (HSQC, ^{1}H,^{1}H-COSY, HMBC, and NOESY) (Figures 6 and S65−S92 and Tables S1 and S3) established the structures of **12** and **13** as depicted in Figure 1. Thus, **12** and **13** were established as two additional new tetracenomycin natural products and named as 8-demethyl-8-*O*-*β*-D-quinovosyl-tetracenomycin C and 8-demethyl-8-*O*-*β*-D-allosyl-tetracenomycin C, respectively. The production of **12** and **13** confirmed the functionality of the construct and also the capability of ElmGT to turn over other 6-deoxysugars. The production of D-quinovose was surprising but not without precedent since the production of D-quinovosyl-narbonolide was reported previously in extracts of *S. venezuelae* ATCC15439 strains in which the *desI*aminotransferase gene had been knocked out.[51] This result could be explained by the action of GerK1 on TDP-4-keto-6-deoxy-D-glucose or possibly by a moonlighting 4-ketoreductase encoded in the host *S. coelicolor* genome.

Next, we decided to test the TDP-D-fucofuranose pathway from the gilvocarcin V biosynthetic gene cluster derived from *S. griseoflavus* Gö3592.[52] Gilvocarcin V is an angucycline-class anticancer antibiotic with an unusual benzo[*d*]-naphthopyranone backbone and a unique *C*-glycosidically linked D-fucofuranose moiety.[53] The gilvocarcin V biosynthetic pathway has been extensively characterized by the Rohr lab over the past two decades,[54−67] including the characterization of the 4-ketoreductase (GilU)[63] responsible for the TDP-D-fucofuranose biosynthetic pathway. Recently, several gilvocarcin-type molecules with modifications to the D-fucofuranose ring have been isolated from soil-derived actinomycetes.[68] However, the enzyme responsible for the unique TDP-D-fucopyranose to TDP-D-fucofuranose ring contraction remains uncharacterized. The TDP-D-fucofuranose pathway from *E. coli* has been characterized, which utilizes a 4-ketoreductase (Fcf1) and a mutase (Fcf2) for the elaboration of the five-membered sugar. In the gilvocarcin biosynthetic pathway, no obvious candidates for the mutase enzyme exist, and only *gilN*, *gilL*, *gilS*, and *gilV* are the remaining orphans for which no role in gilvocarcin biosynthesis has been assigned.[69] GilV was viewed as a potential candidate for the mutase enzyme, given its direct proximity immediately upstream of the gilvocarcin *C*-glycosyltransferase *gilGT*. GilV is a small protein (116 amino acids), and querying the NCBI nr database revealed no identified conserved domains.

We designed a construct expressing *desIII* + *desIV* + *gilU* + *gilV* and transformed this construct into *S. coelicolor* M1146::cos16-F4iE (Table 1). The expression of the construct resulted in the production of two glycosylated tetracenomycins, both with parent mass ions of m/z = 603 $[M - H]^-$, indicating the

https://doi.org/10.1021/acsomega.3c02460
ACS Omega 2023, 8, 21237−21253

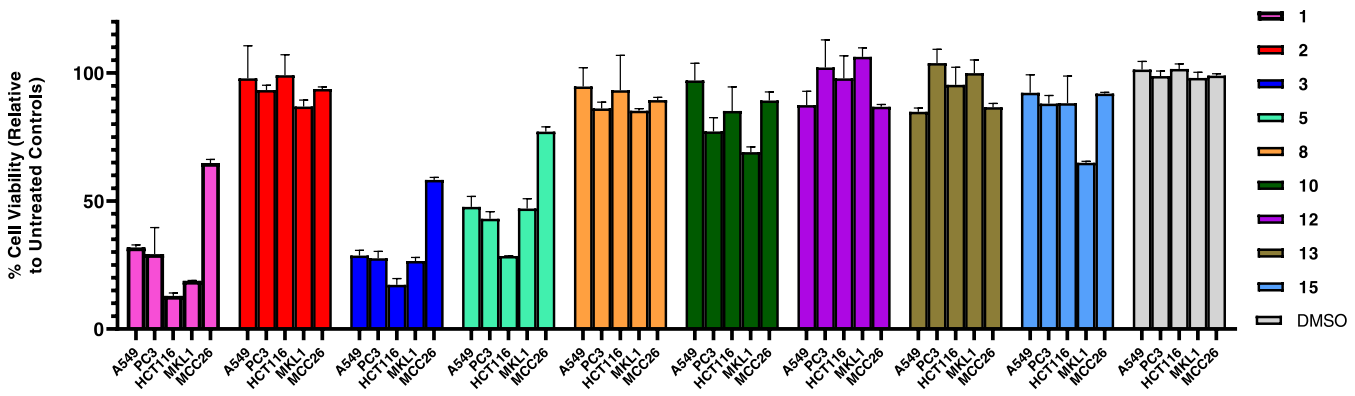

Figure 7. % Viability of A549 (nonsmall lung), PC3 (prostate), and HCT116 (colorectal) human cancer cell lines and Merkel cells (MKL1 and MCC26) (after 72 h) at 80 μM concentration of representative compounds **1**−**3**, **5**, **8**, **10**, **12**, **13**, and **15**. For dose−response curves of the tested compounds, see Figures S3 and S4.

Table 3. Antiproliferative Activities of Compounds 1−3, 5, 8, 10, 12, 13, and 15[a]

compounds	IC_{50} (μM)			IC_{50} (μM)	
	A549	PC3	HCT116	MKL1	MCC26
elloramycin A (**1**)	45.80 ± 39.80	35.90 ± 15.3	16.62 ± 3.43	22.10 ± 1.29	>80
8-demethyltetracenomycin C (**2**)	>80	>80	>80	>80	>80
tetracenomycin C (**3**)	7.13 ± 1.36	2.90 ± 0.90	2.53 ± 0.47	4.91 ± 0.13	29.30 ± 5.41
6-hydroxy-tetracenomycin C (**5**)	59.10 ± 1.14	51.60 ± 26.0	67.90 ± 5.30	63.30 ± 10.80	>80
8-demethyl-8-*O*-β-D-olivosyl-tetracenomycin C (**8**)	>80	>80	>80	>80	>80
8-demethyl-8-*O*-β-D-mycarosyl-TCMC (**10**)	>80	>80	>80	>80	>80
8-demethyl-8-*O*-β-D-quinovosyl-TCMC (**12**)	>80	>80	>80	>80	>80
8-demethyl-8-*O*-β-D-allosyl-TCMC (**13**)	>80	>80	>80	>80	>80
8-demethyl-8-*O*-(2′-methoxy)-α-L-rhamnosyl-TCMC (**15**)	>80	>80	>80	>80	>80

[a]Antiproliferative IC_{50} values were obtained after 72 h incubation. Actinomycin D and H_2O_2 [A549 (nonsmall cell lung), PC3 (prostate), and HCT116 (colorectal) human cancer cell lines and Merkel cells MKL1 and MCC26] were used as a positive control at 20 μM and 1 mM concentration, respectively (0% viable cells, n = 3). Remaining compounds were not tested due to the lack of materials. For dose−response data of the tested compounds, see Figures S3 and S4.

accumulation of two tetracenomycin analogues with appended 6-deoxysugars (Figure 5H). The compounds corresponded to **12** and a new tetracenomycin analogue, 8-demethyl-8-*O*-D-fucosyl-tetracenomycin C (**14**). The chemical structure of **14** was established by HRMS and NMR data analysis. The molecular formula of **14** was deduced as $C_{28}H_{28}O_{15}$ on the basis of (+)-HRESI-MS [m/z 605.1508 $[M + H]^+$ (calcd for $C_{28}H_{29}O_{15}$, 605.1501)], (−)-HRESI-MS [m/z 603.1377 $[M - H]^-$ (calcd for $C_{28}H_{27}O_{15}$, 603.1355)], and NMR data. The comparison of the NMR data of compounds **12** and **14** confirmed that both compounds were only different at the 4′-position of the sugar residues (Tables S1−S4). The coupling constants of H-4′ (δ_H 2.92, t, J = 8.6 Hz) in compound **12** were different from those of H-4′ (δ_H 3.70, dd, J = 3.6 Hz) in compound **14**, confirming the equatorial orientation of H-4′ in compound **14** (H-4′ is equatorial/axial coupled with H-5′/H-3′). All of the remaining 2D NMR (^{1}H,^{1}H-COSY, HMBC, and NOESY) correlations are in full agreement with structure **14** (Figures 6 and S93−S101). Based on the cumulative spectroscopic data, **12** and **14** differed only at the C-4′ stereocenter, and thus, compound **14** (bearing an *O*-β-D-fucosyl residue) is a 4′-*epi* form of **12**. Consistent with the cumulative 1D and 2D NMR data analysis, the structure of **14** was established as a new tetracenomycin analogue, and **14** was named 8-demethyl-8-*O*-β-D-fucosyl-tetracenomycin C (**14**) (Figure 1).

Lastly, we developed a construct encoding biosynthetic pathway of TDP-D-antiarose from the rubterolone A pathway.[70] The rare deoxysugar TDP-D-antiarose features axial 3′-OH and 4′-OH groups, and its formation from TDP-4-keto-6-deoxy-D-glucose is catalyzed by an unusual reductase−epimerase, RubS3 (Figure 4).[70] We generated a construct encoding TDP-D-antiarose biosynthetic pathway (e.g., *desIII* + *desIV* + *rubS3*) (Table 1), but the expression of this construct in *S. coelicolor* M1146::cos16F4iE did not result in the production of any new tetracenomycins. We supposed that the lack of formation of new tetracenomycins was due to the inability of ElmGT to turn over the TDP-D-antiarose sugar.

Tetracenomycin Glycosylation Patterns Influence Bioactivities of the Metabolites. Selected representative compounds **1**−**3**, **5**, **8**, **10**−**13**, and **15** were tested for mammalian cancer cell cytotoxicity [A549 (nonsmall cell lung), PC3 (prostate), and HCT116 (colorectal) human cancer cell lines and Merkel cells (MKL1 and MCC26)] (see the Materials and Methods section, Figures 7, S3, and S4, and Table 3). In the antiproliferation assay, only compounds **1**, **3**, and **5** displayed moderate cytotoxic activities with IC_{50} 2.5−67 μM concentration (Table 3 and Figures S3 and S4). In the single dose assay, compound **2** exhibited essentially no cytotoxicity, which reflects the importance of methyl groups at 8- and 12-positions for antiproliferative activity. Similarly, compound **15** possessed slight activity in the MKL1 cancer cell line but exhibited lower cytotoxicity than **1**. This result indicates that the

https://doi.org/10.1021/acsomega.3c02460
ACS Omega 2023, 8, 21237−21253

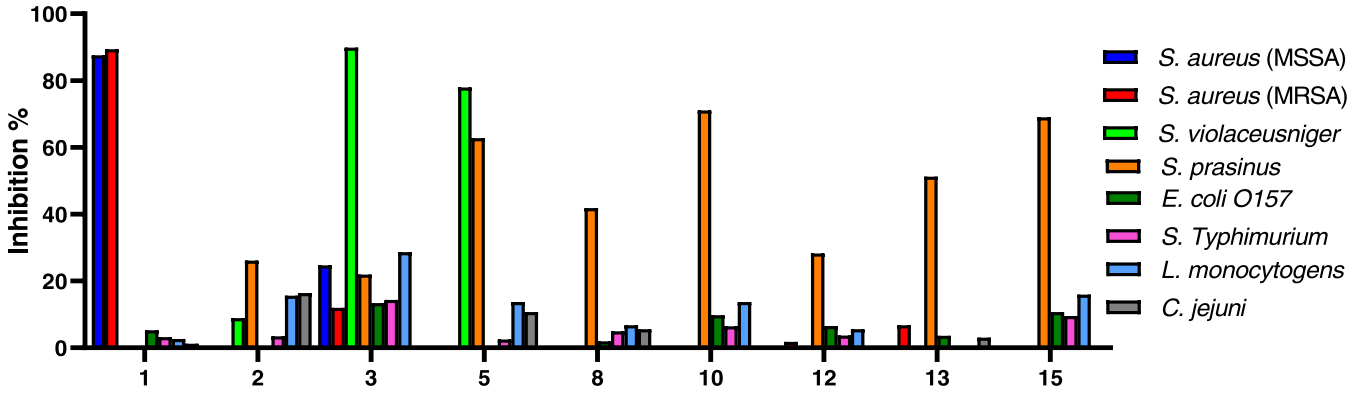

Figure 8. Antibacterial activities of the representative compounds **1**−**3**, **5**, **8**, **10**, **12**, **13**, and **15** (% inhibition). All compounds have been tested at 100 μM concentration against the selected microbial strains. Remaining compounds were not tested due to the lack of materials.

permethylated L-rhamnose of **1** is important for binding and cytotoxicity. Of the compounds that were derived in the present study, compound **10** with the branched D-mycarose sugar exhibited the best activity in the single dose assay in the MKL1 cell line (Figure 7). The glycosylated analogues with neutral glycosides exhibited less cytotoxicity in the cancer cell lines tested. In total, these results indicated that hydrophobic sugars or methyl substitutions at the 8-position may contribute positively to cytotoxicity. Future derivatization efforts could be focused on synthesizing tetracenomycins with alkyl chains or other nonpolar substitutions at the 8-position to develop better ribosome inhibitors with enhanced antiproliferative activity.

In the antibacterial assay, **1** possessed the highest activity against methicillin-susceptible *Staphylococcus aureus* (MSSA; ATCC 12600) and methicillin-resistant *S. aureus* (MRSA; ATCC 43300) (90−95% inhibition, at 100 μM concentration) (Figure 8). This result could indicate that the permethylated L-rhamnose sugar of **1** is indispensable for binding to the nascent polypeptide exit channel of the bacterial 50S ribosome.[14] In addition, it is very exciting that only two compounds (**3** and **5**) inhibited the growth of *Streptomyces violaceusniger* NRRL B-1476 (ATCC 27477) (80−90% inhibition, at 100 μM concentration) (Figure 8). This could indicate that tetracenomycin C analogues without the sugar exhibit some selective inhibition of this strain. Within the set of glycosylated analogues developed in this study, compounds **8**, **10**, **12**, **13**, and **15** exhibited moderately selective inhibition (40−70% inhibition, at 100 μM concentration) of *Streptomyces prasinus* NRRL B-12101 (ATCC 13879), whereas nonglycosylated **2** exhibited comparatively less inhibition (20% inhibition). *S. prasinus* has been shown previously to be susceptible to tetracenomycins.[12,13] Previously, Fiedler et al. described that less methylated derivatives of elloramycin exhibited better antimicrobial activity against Gram-positive bacteria, which agrees with our findings here.[71] While the antibacterial activities of the new derivatives were not so potent, the data presented here provide impetus for further derivation of **1**, e.g., via exploration of additional lipophilic modifications of the L-rhamnose sugar or at the 8-position and the 12-position of tetracenomycin C.

CONCLUSIONS

ElmGT is one of the most successful examples of promiscuous glycosyltransferases useful for combinatorial biosynthesis. The macrolide glycosyltransferases DesVII/DesVIII from *S. venezuelae* and OleD from *S. antibioticus* have also been engineered for several landmark combinatorial biosynthesis and glycorandomization studies, respectively.[72−77] In this work, we leveraged an idempotent BioBricks synthetic biology design to the problem of iterative engineering deoxysugar pathways for combinatorial biosynthesis. The results demonstrate that the BioBricks approach is well-suited for the elaboration of hierarchical deoxysugar pathways, e.g., via the addition or subtraction of dehydratases, ketoreductases, or methyltransferases, target sugar nucleotides can be produced with predictable stereochemistry and structural modifications. In addition, the leveraging of the promiscuous ElmGT and elloramycin biosynthetic pathway provide a ready means for assessing the gene cassettes with efficient throughput. As a result, we were able to reconstitute known pathways in good conversion efficiency (e.g., TDP-D-glucose, TDP-D-olivose, TDP-D-digitoxose, TDP-D-mycarose, TDP-L-rhamnose). We also expanded the chemical diversity of the tetracenomycins with the characterization of a new ketosugar (TDP-4′-keto-D-digitoxose) and new D-series 6-deoxysugars (TDP-D-allose, TDP-D-quinovose, and TDP-D-fucose). In summary, the BioBricks cloning system in *S. coelicolor* M1146::cos16F4iE is an excellent approach for the prototyping of sugar nucleotide pathways *in vivo* and is a launching pad for deeper understanding of structure−activity relationships in this important class of polyketides.

MATERIALS AND METHODS

Bacterial Strains and Growth Conditions. *E. coli* JM109 (Promega) cells were used for routine cloning and maintenance of plasmids. *E. coli* ET12567/pUZ8002 was used as a host for intergeneric conjugation of shuttle vectors with *S. coelicolor*::*cos16F4iE* according to standard procedures (Table 2).[78] *E. coli* JM109 cells and *E. coli* ET12567/pUZ8002 chemically competent cells were prepared using the *E. coli* Mix & Go! Transformation Kit (Zymo Research). Transformation of chemically competent *E. coli* cells was carried out using standard procedures.[79] *E. coli* was routinely grown in lysogeny broth (LB) and on solid LB agar plates. Media were supplemented with antibiotics as necessary: 25 μg/mL apramycin, 25 μg/mL kanamycin, 100 μg/mL ampicillin, and 35 μg/mL chloramphenicol for the growth of *E. coli* strains.

S. coelicolor M1146::cos16F4iE and derivative strains were routinely maintained on solid mannitol soya flour (SFM), DNA, and R5 solid agar plates.[20] *S. coelicolor* M1146::cos16F4iE was used as a genetic host for the expression of "sugar plasmid" expression cassettes. pUWL201PWBB-based plasmids were mobilized into *S. coelicolor* M1146::cos16F4iE via intergeneric

https://doi.org/10.1021/acsomega.3c02460
ACS Omega 2023, 8, 21237−21253

conjugation with *E. coli* ET12567/pUZ8002.[78] In brief, the conjugal mating took place over 16−18 h at 30 °C on solid mannitol soya flour (SFM) agar plates supplemented with 10 mM $MgCl_2$. The conjugation plates were then overlaid with 1.5 mL of sterile water and 50 μg/mL apramycin, 25 μg/mL thiostrepton, and 35 μg/mL nalidixic acid before incubating the plates at 30 °C for 3−4 days until the appearance of exconjugants. Ten to twelve exconjugants per conjugal mating were patch-plated to R5 agar plates supplemented with 50 μg/mL apramycin, 25 μg/mL thiostrepton, and 35 μg/mL nalidixic acid to purify the *S. coelicolor* exconjugants from the *E. coli* conjugal donor cells and grown for an additional 6−7 days at 30 °C.

For liquid cultivations, vegetative mycelia from 10 to 12 independent transformants were scraped from the R5 patch plate, inoculated into 2 mL tryptic soy broth seed cultures, and grown in an orbital shaker at 30 °C and 230 rpm for 24−36 h. The seed cultures (5% v/v inoculum) were inoculated into 50 mL of SG-TES media (20 g/L glucose, 10 g/L Bacto Soytone, 5 g/L yeast extract, 5.73 g/L TES, 1 mg/L cobalt chloride production media). When appropriate, media were supplemented with antibiotics at the following concentrations: 50 μg/mL apramycin, 50 μg/mL hygromycin, 25 μg/mL thiostrepton, and 35 μg/mL nalidixic acid.

Gene Synthesis, DNA Manipulation, and Assembly of BioBricks Vectors. All BioBricks parts were synthesized according to the BioBricks RFC[10] standard.[35] All BioBricks parts were synthesized with the 5′-GAATTCGCGGCCGCTTCTAGAG-3′ BioBricks prefix and the 5′-TACTAGTAGCGGCCGCTGCAG-3′ BioBricks suffix sequences to facilitate cloning. Biosynthetic genes were codon-optimized for expression in *S. coelicolor* and synthesized with the strong BBa_B0034 ribosome binding site in the BioBricks prefix 5′-GAATTCGCGGCCGCTTCTAGAGAAAGAGGAGAAA-TACTAG (underlined) (GenScript). All genetic parts were ordered as synthetic BioBricks genes cloned into the *EcoRI*/*PstI*sites pUC57. Gene cassettes were assembled in construction plasmids pSB1C3-J04450, pSB1K3-J04450, and pSB1A3-J04450 using the *EcoRI, XbaI, SpeI,* and *PstI* restriction sites. Restriction enzymes and T4 DNA ligase were purchased from New England Biolabs. All molecular biology experiments were carried out as previously described.[79]

Isolation and Analysis of Glycosylated Tetracenomycins. Fermentations of *S. coelicolor* M1146::cos16F4iE and derivative strains were carried out in triplicate 50 mL shake flasks of SG media for 5−7 days as previously described.[12] To extract glycosylated tetracenomycins, 25 mL of culture was extracted with 25 mL of ethyl acetate + 0.1% formic acid in a 50 mL conical tube. The organic phase was collected and concentrated in a rotary evaporator. The red-orange residue was resuspended in 4 mL of methanol and filtered, and a 10 μL was sampled via HPLC-MS analysis. Analyses and quantification of tetracenomycins were carried out on an Agilent 1260 Infinity II LC/MSD iQ single quadrupole instrument. In brief, 10 μL of the sample was injected via an autosampler onto the sample loop and was separated on a Poroshell 120 Phenyl-Hexyl column (ID 2.7 μm, 4.6 mm × 100 mm) and was analyzed in gradients of solvent A (0.1% formic acid in water) and solvent B (0.1% formic acid in acetonitrile). The HPLC program used a constant flow rate of 0.5 mL/min and the following gradient steps: 0 min, 95% solvent A and 5% solvent B; 0−10 min, 95% solvent A and 5% solvent B to 5% solvent A and 95% solvent B; 10−13 min, held at 5% solvent A and 95% solvent B; 13.1 min, re-equilibrate to 95% solvent A and 5% solvent B; and 13.1−15.1 min, 95% solvent A and 5% solvent B. The diode array detector (DAD) was set to monitor UV−vis absorbance at 290 and 410 nm. The ESI-MS was set to scan from 200 to 1000 m/z fragments in positive and negative ionization modes. Single ion monitoring was set up in ESI-MS negative ionization mode using the following ions: **1** m/z = 659 $[M - H]^-$; **2** m/z = 457 $[M - H]^-$; **3** m/z = 471 $[M - H]^-$; **4** m/z = 485 $[M - H]^-$; **5** m/z = 487 $[M - H]^-$; **6** m/z = 501 = $[M - H]^-$; **7** m/z = 619 $[M - H]^-$; **8** m/z = 587 $[M - H]^-$; **9** m/z = 587 $[M - H]^-$; **10** m/z = 601 $[M - H]^-$; **11** = m/z = 585 $[M - H]^-$ (keto form), m/z = 603 $[M - H]^-$ (hydrate form); **12** m/z = 603 $[M - H]^-$; **13** m/z = 603 $[M - H]^-$; and **14** m/z = 603 $[M - H]^-$.

General Experimental Procedures. Ultraviolet−visible (UV−vis) spectra were taken directly from analytical HPLC runs and show relative intensities. NMR spectra were recorded at 600 MHz (14.1 T) using a Bruker Avance Neo console equipped with a TCI 5-mm cryoprobe or 500 MHz Bruker AVANCE-III system with liquid nitrogen cooled Prodigy BBO cryoprobe (all spectra were processed in Bruker Topspin 4.1.3 version, and 2D spectra were apodized with QSINE or SINE window functions and zero-filled to 256 × 1024 points), and spectra were analyzed and plotted using Mnova [where δ-values were referenced to respective solvent signals (CD_3OD, δ_H 3.31 ppm, δ_C 49.15 ppm; dimethyl sulfoxide (DMSO)-d_6, δ_H 2.50 ppm, δ_C 39.51 ppm; acetone-d_6, δ_H 2.05 ppm, δ_C 29.92/206.68 ppm) or tetramethylsilane] (Bruker BioSpin Corporation, Billerica, MA). High-resolution electrospray ionization (HRESI) mass spectra were recorded on a AB SCIEX Triple TOF 5600 system or on a Bruker Daltonics micrOTOF system.

HPLC−UV/MS analyses were accomplished with an Agilent InfinityLab LC/MSD mass spectrometer (MS model G6125B; Agilent Technologies, Santa Clara, CA) equipped with an Agilent 1260 Infinity II Series Quaternary LC system and a Phenomenex NX-C18 column (250 × 4.6 mm^2, 5 μm) [method: solvent A: H_2O/0.1% formic acid, solvent B: CH_3CN; flow rate: 0.5 mL/min; 0−30 min, 5−100% B (linear gradient); 30−35 min, 100% B; 35−36 min, 100−5% B; 36−40 min, 5% B]. HPLC−UV analyses were carried out in an Agilent 1260 system equipped with a photodiode array detector (PDA) and a Phenomenex C_{18} column (Phenomenex, Torrance, CA; 250 × 4.6 mm^2, 5 μm; solvent A: H_2O/0.1% trifluoroacetic acid (TFA), solvent B: CH_3CN; flow rate: 1.0 mL/min; 0−30 min, 5−100% B; 30−35 min, 100% B; 35−36 min, 100−5% B; 36−40 min, 5% B) or using a Shimadzu Nexera X3 system equipped with a photodiode array detector and a Kinetex C18 column (1.7 μm, 100 Å, 100 × 2.1 mm^2, Phenomenex) [method: solvent A: H_2O/0.1% TFA; solvent B: CH_3CN; flow rate: 0.3 mL/min; 0−2 min, 0% B; 2−22 min, 0−100% B; 22−24 min, 100% B; 24−29 min, 0% B]. Semipreparative HPLC were carried out in an Agilent 1260 Infinity II (prep-HPLC) system equipped with a diode array detector (DAD) and a Gemini 5 μm C_{18} 110 Å, LC column 250 × 10 mm^2 (Phenomenex, Torrance, CA) [method A: H_2O/0.025% TFA; solvent B: CH_3CN; flow rate: 5.0 mL/min; 0−2 min, 15% B; 2−31 min, 15−100% B; 31−33 min, 100% B; 33−34 min, 100−15% B; 34−36 min, 10% B; method B: solvent A: H_2O/0.025% TFA; solvent B: CH_3CN; flow rate: 5.0 mL/min; 0−2 min, 15% B; 2−28 min, 15−75% B; 28−30 min 75−100% B; 30−32 min, 100% B; 32−34 min, 100−15% B; 34−36 min, 15% B] or using a LC-20AP/CBM-20A system with a diode array detector (Shimadzu) and EVO C18, 5 μm, 100 Å, 250 × 21.2 mm^2 Kinetex column (Phenomenex) [method C: solvent A: H_2O/0.1% TFA; solvent B: CH_3CN; flow rate: 20

https://doi.org/10.1021/acsomega.3c02460
ACS Omega 2023, 8, 21237−21253

mL/min; 0−2 min, 0% B; 2−22 min, 0−100% B; 22−24 min, 100% B; 24−29 min, 0% B; method D: solvent A: 50% 60 mM ammonium acetate−acetic acid pH 3.6, 15% CH_3CN, 35% H_2O; solvent B: CH_3CN; flow rate: 20 mL/min; 0−2 min, 0% B; 2−20 min, 0−60% B; 20−24 min, 100% B; 24−29 min, 0% B]. All solvents used were of ACS grade and purchased from the Pharmco-AAPER (Brookfield, CT). Size-exclusion chromatography was performed on Sephadex LH-20 (MeOH; 25−100 μm; GE Healthcare, Piscataway, NJ). Silica chromatography was performed using high-purity grade silica (pore size 60 Å, 230−400 mesh particle size) and a gradient elution from 99:0:1 $CHCl_3$/MeOH/HCOOH to 0:99:1 $CHCl_3$/MeOH/HCOOH. A549, PC3, and HCT116 cells and all of the microbial strains tested in this study were obtained from ATCC (Manassas, VA). All other reagents used were reagent grade and purchased from Sigma-Aldrich (Saint Louis, MO) unless stated otherwise.

Purification of Compounds 1, 2, 8, 10, 12, and 13. *S. coelicolor* M1146::cos16F4iE/pDOLV, *S. coelicolor* M1146::cos16F4iE/pDMYC, *S. coelicolor* M1146::cos16F4iE/pDFUCO2, *S. coelicolor* M1146::cos16F4iE/pDALO were cultured in 4 L of SG-TES liquid media (100 mL × 40 shake flasks, 250 mL Erlenmeyer baffled flask) in an orbital shaker at 220 rpm for 5−6 days. The resulting cells were centrifuged at 3000 rpm for 10 min, and the cell pellet was extracted in 1 L of methanol. The fermentation broth was extracted 3 times with 4 L of ethyl acetate + 0.1% formic acid. The fractions were filtered, combined, and then dried *in vacuo*. The resulting extract was dissolved in 9:1 chloroform/methanol, dry-loaded on a 25 g silica cartridge, and fractionated on a silica cartridge (24 g silica RediSep Rf Gold) on a Teledyne Combiflash 100 instrument using a gradient of chloroform to 9:1 chloroform/methanol at a flow rate of 30 mL/min over 15 min. The resulting fractions were dried down and polished via prep-HPLC. The obtained fraction *F*1 was purified by prep-HPLC using method A afforded 8-demethyl-8-*O*-β-D-mycarosyl-tetracenomycin C (**10**) and 8-demethyl-tetracenomycin C (**2**) in pure form as yellow solids. Similarly, fraction *F*2 was subjected for chromatographic purification using Sephadex LH-20 (MeOH; 2.0 × 30 cm^2), followed by *prep*-HPLC (method A) to afford 8-demethyl-8-β-D-olivosyl-tetracenomycin C (**8**) in pure form as a yellow solid. On the same manner, *prep*-HPLC purification using method B afforded compounds **1**, **12**, and **13** in pure form.

Growth Conditions and Isolation of Compounds 7, 9, 11, and 14. *S. coelicolor* M1146/cos16F4iE transformants were grown on mannitol soya flour (MS) plates (mannitol 20 g/L, soya flour 20 g/L, agar 20 g/L) supplemented with thiostrepton and apramycin at +30 °C for 5 days. The resulting *S. coelicolor* M1146/cos16F4iE transformant spores were used to inoculate 250 mL Erlenmeyer flasks containing 50 mL of E1 media (glucose 20 g/L, starch 20 g/L, cottonseed flour 5 g/L, yeast extract 2.5 g/L, $K_2HPO_4{\cdot}3H_2O$ 1.3 g/L, $MgSO_4{\cdot}7H_2O$ 1 g/L, NaCl 3 g/L, $CaCO_3$ 3 g/L) supplemented with thiostrepton and apramycin and incubated for 3 days (+30 °C, 300 rpm). This seed culture was used to inoculate (4% v/v) 2 L Erlenmeyer flasks containing 250 mL of E1 media supplemented with thiostrepton and apramycin, which were incubated for 7 days (+30 °C, 250 rpm). Compounds were extracted from cultures by adding 20 g/L LXA-1180 resin (SUNRESIN) and incubating overnight (180 rpm, +30 °C). The LXA-1180 resin was separated from the culture, and the compounds were eluted with methanol. Methanol was evaporated using a rotary evaporator, and compounds were resuspended in a minimal volume of methanol.

Purification of Compounds 7, 11, and 14. Methanol extracts from cultures were first purified by silica chromatography. Fractions from silica chromatography containing compounds of interest were evaporated using a rotary evaporator and suspended in a minimal volume of methanol for semipreparative HPLC with method C for 8-demethyl-8-*O*-β-D-fucosyl-tetracenomycin C (**14**) and method D for 8-demethyl-8-*O*-β-D-glucosyl-tetracenomycin C (**7**) and 8-demethyl-8-*O*-(4′-keto)-β-D-digitoxosyl-tetracenomycin C (**11**). Fractions containing pure compounds were extracted with ethyl acetate, dried using a rotary evaporator and desiccator, and resuspended in deuterated solvents for NMR measurements.

Purification of 8-Demethyl-8-*O*-β-D-digitoxosyl-tetracenomycin C (9). Methanol extracts from cultures were first purified by size-exclusion chromatography using Sephadex LH-20. Fractions containing compounds of interest were evaporated using a rotary evaporator and suspended in minimal volume of methanol for semipreparative HPLC with method D. Fractions containing pure compounds were extracted with ethyl acetate, dried using a rotary evaporator and desiccator, and resuspended in deuterated solvents for NMR measurements.

Cancer Cell Line Viability Assay. Mammalian cell line cytotoxicity [A549 (nonsmall cell lung), PC3 (prostate), and HCT116 (colorectal) human cancer cell lines and Merkel cells MKL1 and MCC26] assays were accomplished in triplicate following our previously reported protocols.[80−83] Vehicle (DMSO) was used as the negative control, and actinomycin D and H_2O_2 (A549 and PC3; MKL1 and MCC26) were used as positive controls at 20 μM and 1 mM concentration, respectively.

Antibacterial Assay. To assess the antimicrobial efficacy of the compounds, we tested their effect on the growth of pathogenic bacteria using the microdilution well assay and grown the bacteria as previously described[84−87] Briefly, *E. coli* O157:H7 (ATCC 35150), *Salmonella enterica* serovar Typhimurium (ATCC 14028), *Listeria monocytogenes* (ATCC 15313), and methicillin-susceptible *S. aureus* (MSSA; ATCC 12600), methicillin-resistant *S. aureus* (MRSA; ATCC 43300) were grown in Luria Bertani (LB) media overnight at 37 °C for 12 h, while *Campylobacter jejuni* 81−176 (ATCC 33560) was grown in Muller Hinton (MH) media at 42 °C for 48 h. *S. prasinus* NRRL B-12101 (ATCC 13879) and *S. violaceusniger* NRRL B-1476 (ATCC 27477) were grown in ISP broth. Hundred microliters of each bacterial culture (0.05 OD_{600}; approximately 1×10^7 CFU/mL) were grown in the presence of 1 μL of each compound (100 μM final concentration) in the respective media using a 96-well plate. DMSO, 1 μL of chloramphenicol (20 μg/mL), and culture media of each bacterium were used as controls.

Physicochemical Properties of Compounds 1−2 and 7−14. *Elloramycin A (1).* $C_{32}H_{36}O_{15}$ (660); yellow solid; HPLC-R_t = 24.84 min (Figure S6); UV/vis λ_{max} 210, 258 (sh), 288, 394 (sh), 410 nm; ^{1}H NMR (CD_3OD, 600 MHz) and ^{13}C NMR (CD_3OD, 150 MHz), see Tables S1 and S3 (Supporting Information); (−)-ESI-MS: *m*/*z* 659 $[M - H]^-$; (+)-ESI-MS: *m*/*z* 661 $[M + H]^+$, 473 $[(M\text{-sugar}) + H]^+$; (+)-HRESI-MS: *m*/*z* 661.2127 $[M + H]^+$ (calcd for $C_{32}H_{37}O_{15}$, 661.2127), 1338.4420 $[2M + NH_4]^+$ (calcd for $C_{64}H_{76}O_{30}N$, 1338.4446).

8-Demethyl-tetracenomycin C (2). $C_{22}H_{18}O_{11}$ (458); yellow solid; HPLC-R_t = 19.95 min (Figure S16); UV/vis λ_{max} 216, 252 (sh), 290, 396 (sh), 412 nm; ^{1}H NMR (CD_3OD, 600 MHz) and ^{13}C NMR (CD_3OD, 150 MHz), see Tables S1 and S3

https://doi.org/10.1021/acsomega.3c02460
ACS Omega 2023, 8, 21237−21253

(Supporting Information); (−)-ESI-MS: m/z 457 $[M - H]^-$; (+)-ESI-MS: m/z 459 $[M + H]^+$.

8-Demethyl-8-O-β-D-glucosyl-tetracenomycin C (7). $C_{28}H_{28}O_{16}$ (620); yellow solid; HPLC-R_t = 16.06 min (Figure S24); UV/vis λ_{max} 214, 244 (sh), 286, 394 (sh), 410 nm; ^{1}H NMR (CD_3OD, 600 MHz) and ^{13}C NMR (CD_3OD, 150 MHz), see Tables S2 and S4 (Supporting Information); (−)-ESI-MS: m/z 619 $[M - H]^-$; (+)-ESI-MS: m/z 459 [(M-sugar) + H]$^+$; (+)-HRESI-MS: m/z 621.1454 $[M + H]^+$ (calcd for $C_{28}H_{29}O_{16}$, 621.1450), 459.0925 [(M-sugar) + H]$^+$ (calcd for $C_{22}H_{19}O_{11}$, 459.0922); (−)-HRESI-MS: m/z 619.1305 $[M - H]^-$ (calcd for $C_{28}H_{27}O_{16}$, 619.1305), 1239.2682 $[2M - H]^-$ (calcd for $C_{56}H_{55}O_{32}$, 1239.2682).

8-Demethyl-8-O-β-D-olivosyl-tetracenomycin C (8). $C_{28}H_{28}O_{14}$ (588); yellow solid; HPLC-R_t = 18.63 min (Figure S34); UV/vis λ_{max} 214, 240 (sh), 286, 394 (sh), 410 nm; ^{1}H NMR (CD_3OD, 600 MHz) and ^{13}C NMR (CD_3OD, 150 MHz), see Tables S1 and S3 (Supporting Information); (−)-ESI-MS: m/z 587 $[M - H]^-$; (+)-ESI-MS: m/z 589 $[M + H]^+$, 459 [(M-sugar) + H]$^+$.

8-Demethyl-8-O-β-D-digitoxosyl-tetracenomycin C (9). $C_{28}H_{28}O_{14}$ (588); yellow solid; ^{1}H NMR (acetone-d_6, 500 MHz) and ^{13}C NMR (acetone-d_6, 125 MHz), see Tables S2 and S4 (Supporting Information); (−)-HRESI-MS: m/z 587.1384 $[M - H]^-$ (calcd for $C_{28}H_{27}O_{14}$, 587.1406), 1175.2886 $[2M - H]^-$ (calcd for $C_{56}H_{55}O_{28}$, 1175.2885).

8-Demethyl-8-O-β-D-mycarosyl-tetracenomycin C (10). $C_{29}H_{30}O_{14}$ (602); yellow solid; HPLC-R_t = 20.37 min (Figures S47 and S48); UV/vis λ_{max} 216, 244 (sh), 286, 394 (sh), 410 nm; ^{1}H NMR (CD_3OD, 600 MHz) and ^{13}C NMR (CD_3OD, 150 MHz), see Tables S1 and S3 (Supporting Information); (−)-ESI-MS: m/z 601 $[M - H]^-$; (+)-ESI-MS: m/z 603 $[M + H]^+$, 459 [(M-sugar) + H]$^+$.

8-Demethyl-8-O-(4′-keto)-β-D-digitoxosyl-tetracenomycin C (11). $C_{28}H_{26}O_{14}$ (586); yellow solid; HPLC-R_t = 22.97 min (Figure S55); UV/vis λ_{max} 210, 240 (sh), 286, 392 (sh), 408 nm; ^{1}H NMR (acetone-d_6, 600 MHz) and ^{13}C NMR (acetone-d_6, 125 MHz), see Tables S2 and S4 (Supporting Information); (−)-ESI-MS: m/z 585 $[M - H]^-$; (+)-ESI-MS: m/z 587 $[M + H]^+$, 459 [(M-sugar) + H]$^+$; (+)-HRESI-MS: m/z 587.1385 $[M + H]^+$ (calcd for $C_{28}H_{27}O_{14}$, 587.1395), 459.0906 [(M-sugar) + H]$^+$ (calcd for $C_{22}H_{19}O_{11}$, 459.0922); (−)-HRESI-MS: m/z 585.1250 $[M - H]^-$ (calcd for $C_{28}H_{25}O_{14}$, 585.1250), 1171.2593 $[2M - H]^-$ (calcd for $C_{56}H_{51}O_{28}$, 1171.2572).

8-Demethyl-8-O-β-D-quinovosyl-tetracenomycin C (12). $C_{28}H_{28}O_{15}$ (604); yellow solid; HPLC-R_t = 17.27 min (Figures S65 and S66); UV/vis λ_{max} 210, 250 (sh), 286, 394 (sh), 410 nm; ^{1}H NMR (CD_3OD and DMSO-d_6, 600 MHz) and ^{13}C NMR (CD_3OD and DMSO-d_6, 150 MHz), see Tables S1 and S3 (Supporting Information); (−)-ESI-MS: m/z 603 $[M - H]^-$; (+)-ESI-MS: m/z 605 $[M + H]^+$, 459 [(M-sugar) + H]$^+$; (+)-HRESI-MS: m/z 605.1504 $[M + H]^+$ (calcd for $C_{28}H_{29}O_{15}$, 605.1501), 459.0924 [(M-sugar) + H]$^+$ (calcd for $C_{22}H_{19}O_{11}$, 459.0922), 1226.3197 $[2M + NH_4]^+$ (calcd for $C_{56}H_{60}O_{30}N$, 1226.3194).

8-Demethyl-8-O-β-D-allosyl-tetracenomycin C (13). $C_{28}H_{28}O_{15}$ (604); yellow solid; HPLC-R_t = 17.76 min (Figures S82 and S83); UV/vis λ_{max} 210, 258 (sh), 288, 394 (sh), 410 nm; ^{1}H NMR (DMSO-d_6, 600 MHz) and ^{13}C NMR (DMSO-d_6, 150 MHz), see Tables S1 and S3 (Supporting Information); (−)-ESI-MS: m/z 603 $[M - H]^-$; (+)-ESI-MS: m/z 605 $[M + H]^+$, 459 [(M-sugar) + H]$^+$; (+)-HRESI-MS: m/z 605.1501 $[M + H]^+$ (calcd for $C_{28}H_{29}O_{15}$, 605.1501), 459.0921 [(M-sugar) + H]$^+$ (calcd for $C_{22}H_{19}O_{11}$, 459.0922), 1226.3166 $[2M + NH_4]^+$ (calcd for $C_{56}H_{60}O_{30}N$, 1226.3194).

8-Demethyl-8-O-β-D-fucosyl-tetracenomycin C (14). $C_{28}H_{28}O_{15}$ (604); yellow solid; HPLC-R_t = 16.64 min (Figure S93); UV/vis λ_{max} 212, 238 (sh), 288, 394 (sh), 410 nm; ^{1}H NMR (CD_3OD, 500 MHz) and ^{13}C NMR (CD_3OD, 125 MHz), see Tables S2 and S4 (Supporting Information); (−)-ESI-MS: m/z 603 $[M - H]^-$; (+)-ESI-MS: m/z 605 $[M + H]^+$, 459 [(M-sugar) + H]$^+$; (+)-HRESI-MS: m/z 605.1508 $[M + H]^+$ (calcd for $C_{28}H_{29}O_{15}$, 605.1501), 459.0949 [(M-sugar) + H]$^+$ (calcd for $C_{22}H_{19}O_{11}$, 459.0922); 1226.3220 $[2M + NH_4]^+$ (calcd for $C_{56}H_{55}O_{30}$, 1226.3194); (−)-HRESI-MS: m/z 603.1377 $[M - H]^-$ (calcd for $C_{28}H_{27}O_{15}$, 603.1355), 1207.2776 $[2M - H]^-$ (calcd for $C_{56}H_{55}O_{30}$, 1207.2784).

■ ASSOCIATED CONTENT

Supporting Information

The Supporting Information is available free of charge at https://pubs.acs.org/doi/10.1021/acsomega.3c02460.

High-resolution mass spectrometry data, NMR tables, NMR spectra, HPLC−UV−vis chromatograms, antimicrobial activity, dose−response data for human cancer cell lines, and sequences of *oleL* and *oleU* (PDF)

■ AUTHOR INFORMATION

Corresponding Authors

S. Eric Nybo − *Department of Pharmaceutical Sciences, College of Pharmacy, Ferris State University, Big Rapids, Michigan 49307, United States;* orcid.org/0000-0001-7884-7787; Email: EricNybo@Ferris.edu

Mikko Metsä-Ketelä − *Department of Life Technologies, University of Turku, FIN-20014 Turku, Finland;* orcid.org/0000-0003-3176-2908; Email: mianme@utu.fi

Khaled A. Shaaban − *Center for Pharmaceutical Research and Innovation, College of Pharmacy, University of Kentucky, Lexington, Kentucky 40536, United States; Department of Pharmaceutical Sciences, College of Pharmacy, University of Kentucky, Lexington, Kentucky 40536, United States;* orcid.org/0000-0001-7638-4942; Email: Khaled_shaaban@uky.edu

Authors

Heli Tirkkonen − *Department of Life Technologies, University of Turku, FIN-20014 Turku, Finland;* orcid.org/0000-0002-9913-226X

Katelyn V. Brown − *Department of Pharmaceutical Sciences, College of Pharmacy, Ferris State University, Big Rapids, Michigan 49307, United States*

Magdalena Niemczura − *Department of Life Technologies, University of Turku, FIN-20014 Turku, Finland*

Zélie Faudemer − *Chemistry and Chemical Engineering Department, SIGMA Clermont, 63170 Aubière, France*

Courtney Brown − *Department of Pharmaceutical Sciences, College of Pharmacy, Ferris State University, Big Rapids, Michigan 49307, United States*

Larissa V. Ponomareva − *Center for Pharmaceutical Research and Innovation, College of Pharmacy, University of Kentucky, Lexington, Kentucky 40536, United States; Department of Pharmaceutical Sciences, College of Pharmacy, University of Kentucky, Lexington, Kentucky 40536, United States*

https://doi.org/10.1021/acsomega.3c02460
ACS Omega 2023, 8, 21237−21253

Yosra A. Helmy − *Department of Veterinary Science, College of Agriculture, Food, and Environment, University of Kentucky, Lexington, Kentucky 40546, United States*

Jon S. Thorson − *Center for Pharmaceutical Research and Innovation, College of Pharmacy, University of Kentucky, Lexington, Kentucky 40536, United States; Department of Pharmaceutical Sciences, College of Pharmacy, University of Kentucky, Lexington, Kentucky 40536, United States;* orcid.org/0000-0002-7148-0721

Complete contact information is available at: https://pubs.acs.org/10.1021/acsomega.3c02460

Notes

The authors declare no competing financial interest.

■ ACKNOWLEDGMENTS

Research reported in this publication was supported by the National Science Foundation under Grant No. ENG-2015951 (S.E.N.), the National Cancer Institute of the National Institutes of Health under Award No. R15CA252830 (S.E.N.), the National Institutes of Health grant R37 AI052218, the Center of Biomedical Research Excellence (COBRE) in Pharmaceutical Research and Innovation (CPRI, NIH P20 GM130456), the University of Kentucky College of Pharmacy, the National Center for Advancing Translational Sciences (UL1TR000117 and UL1TR001998), the National Institutes of Health shared instrumentation grant (S10OD28690), Novo Nordisk Foundation Grant No. NNF19OC0057511 (to M.M.-K.), and Academy of Finland Grant No. 340013 (to M.M.-K.). The authors also acknowledge a grant from the Turku University Foundation. They thank the College of Pharmacy NMR Center (University of Kentucky) for NMR support and thank Prof. Dr. Mervyn Bibb (John Innes Centre, Norwich, U.K.) for the gift of strain *S. coelicolor* M1146. They also thank Dr. Isaac Brownell (Dermatology Branch, National Cancer Institute, National Institutes of Health, Bethesda, MD) for the gift of Merkel cells MKL1 and MCC26.

■ REFERENCES

(1) Liang, D.-M.; Liu, J.-H.; Wu, H.; Wang, B.-B.; Zhu, H.-J.; Qiao, J.-J. Glycosyltransferases: Mechanisms and Applications in Natural Product Development. *Chem. Soc. Rev.* **2015**, *44*, 8350−8374.

(2) Thibodeaux, C. J.; Melancon, C. E.; Liu, H. W. Natural-Product Sugar Biosynthesis and Enzymatic Glycodiversification. *Angew. Chem., Int. Ed.* **2008**, *47*, 9814−9859.

(3) Huang, G.; Lv, M.; Hu, J.; Huang, K.; Xu, H. Glycosylation and Activities of Natural Products. *Mini-Rev. Med. Chem.* **2016**, *16*, 1013−1016.

(4) Thorson, J. S.; Vogt, T. Glycosylated Natural Products. *Carbohydrate-Based Drug Discovery*; Wiley-VCH Verlag GmbH & Co. KGaA: Weinheim, 2005; pp 685−711.

(5) Elshahawi, S. I.; Shaaban, K. A.; Kharel, M. K.; Thorson, J. S. A Comprehensive Review of Glycosylated Bacterial Natural Products. *Chem. Soc. Rev.* **2015**, *44*, 7591−7697.

(6) Salas, J. A.; Méndez, C. Engineering the Glycosylation of Natural Products in Actinomycetes. *Trends Microbiol.* **2007**, 219−232.

(7) Thibodeaux, C. J.; Melancon, C. E.; Liu, H. Unusual Sugar Biosynthesis and Natural Product Glycodiversification. *Nature* **2007**, *446*, 1008−1016.

(8) Rodríguez, L.; Aguirrezabalaga, I.; Allende, N.; Braña, A. F.; Méndez, C.; Salas, J. A. Engineering Deoxysugar Biosynthetic Pathways from Antibiotic-Producing Microorganisms: A Tool to Produce Novel Glycosylated Bioactive Compounds. *Chem. Biol.* **2002**, *9*, 721−729.

(9) Lombó, F.; Gibson, M.; Greenwell, L.; Braña, A. F.; Rohr, J.; Salas, J. A.; Méndez, C. Engineering Biosynthetic Pathways for Deoxysugars: Branched-Chain Sugar Pathways and Derivatives from the Antitumor Tetracenomycin. *Chem. Biol.* **2004**, *11*, 1709−1718.

(10) Pérez, M.; Lombó, F.; Baig, I.; Braña, A. F.; Rohr, J.; Salas, J. A.; Méndez, C. Combinatorial Biosynthesis of Antitumor Deoxysugar Pathways in *Streptomyces griseus*: Reconstitution of "Unnatural Natural Gene Clusters" for the Biosynthesis of Four 2,6-D-Dideoxyhexoses. *Appl. Environ. Microbiol.* **2006**, *72*, 6644−6652.

(11) Pérez, M.; Lombó, F.; Zhu, L.; Gibson, M.; Braña, A. F.; Rohr, J.; Salas, J. A.; Méndez, C. Combining Sugar Biosynthesis Genes for the Generation of L- and D-Amicetose and Formation of Two Novel Antitumor Tetracenomycins. *Chem. Commun.* **2005**, 1604−1606.

(12) Eric Nybo, S.; Shabaan, K. A.; Kharel, M. K.; Sutardjo, H.; Salas, J. A.; Méndez, C.; Rohr, J. Ketoolivosyl-Tetracenomycin C: A New Ketosugar Bearing Tetracenomycin Reveals New Insight into the Substrate Flexibility of Glycosyltransferase ElmGT. *Bioorg. Med. Chem. Lett.* **2012**, *22*, 2247−2250.

(13) Zeeck, A.; Reuschenbach, P.; Zähner, H.; Rohr, J. Metabolic Products of Microorganisms. 225. Elloramycin, a New Anthracycline-like Antibiotic from *Streptomyces olivaceus* Isolation, Characterization, Structure and Biological Properties. *J. Antibiot.* **1985**, *38*, 1291−1301.

(14) Osterman, I. A.; Wieland, M.; Maviza, T. P.; Lashkevich, K. A.; Lukianov, D. A.; Komarova, E. S.; Zakalyukina, Y. V.; Buschauer, R.; Shiriaev, D. I.; Leyn, S. A.; Zlamal, J. E.; Biryukov, M. V.; Skvortsov, D. A.; Tashlitsky, V. N.; Polshakov, V. I.; Cheng, J.; Polikanov, Y. S.; Bogdanov, A. A.; Osterman, A. L.; Dmitriev, S. E.; Beckmann, R.; Dontsova, O. A.; Wilson, D. N.; Sergiev, P. V. Tetracenomycin X Inhibits Translation by Binding within the Ribosomal Exit Tunnel. *Nat. Chem. Biol.* **2020**, *16*, 1071−1077.

(15) Decker, H.; Haag, S. Cloning and Characterization of a Polyketide Synthase Gene from *Streptomyces fradiae* Tü2717, Which Carries the Genes for Biosynthesis of the Angucycline Antibiotic Urdamycin A and a Gene Probably Involved in Its Oxygenation. *J. Bacteriol.* **1995**, *177*, 6126−6136.

(16) Alferova, V. A.; Maviza, T. P.; Biryukov, M. V.; Zakalyukina, Y. V.; Lukianov, D. A.; Skvortsov, D. A.; Vasilyeva, L. A.; Tashlitsky, V. N.; Polshakov, V. I.; Sergiev, P. V.; Korshun, V. A.; Osterman, I. A. Biological Evaluation and Spectral Characterization of a Novel Tetracenomycin X Congener. *Biochimie* **2022**, *192*, 63−71.

(17) Weber, W.; Zähner, H.; Siebers, J.; Schröder, K.; Zeeck, A. Stoffwechselprodukte von Mikroorganismen. 175. Mitteilung. Tetracenomycin C. *Arch. Microbiol.* **1979**, *121*, 111−116.

(18) Egert, E.; Noltemeyer, M.; Siebers, J.; Rohr, J.; Zeeck, A. The Structure of Tetracenomycin C. *J. Antibiot.* **1992**, *45*, 1190−1192.

(19) Yue, S.; Motamedi, H.; Wendt-Pienkowski, E.; Hutchinson, C. R. Anthracycline metabolites of tetracenomycin C-nonproducing *Streptomyces glaucescens* mutants. *J. Bacteriol.* **1986**, *167*, 581−586.

(20) Decker, H.; Rohr, J.; Motamedi, H.; Zähner, H.; Hutchinson, C. R. R. Identification of *Streptomyces olivaceus* Tü 2353 Genes Involved in the Production of the Polyketide Elloramycin. *Gene* **1995**, *166*, 121−126.

(21) Ramos, A.; Lombo, F.; Brana, A. F.; Rohr, J.; Mendez, C.; Salas, J. A. Biosynthesis of Elloramycin in *Streptomyces olivaceus* Requires Glycosylation by Enzymes Encoded Outside the Aglycon Cluster. *Microbiology* **2008**, *154*, 781−788.

(22) Nguyen, J. T.; Riebschleger, K. K.; Brown, K. V.; Gorgijevska, N. M.; Nybo, S. E. A BioBricks Toolbox for Metabolic Engineering of the Tetracenomycin Pathway. *Biotechnol. J.* **2022**, *17*, No. 2100371.

(23) Fischer, C.; Rodríguez, L.; Patallo, E. P.; Lipata, F.; Braña, A. F.; Méndez, C.; Salas, J. A.; Rohr, J. Digitoxosyltetracenomycin C and Glucosyltetracenomycin C, Two Novel Elloramycin Analogues Obtained by Exploring the Sugar Donor Substrate Specificity of Glycosyltransferase ElmGT. *J. Nat. Prod.* **2002**, *65*, 1685−1689.

(24) Decker, H.; Haag, S.; Udvarnoki, G.; Rohr, J. Novel Genetically Engineered Tetracenomycins. *Angew. Chem., Int. Ed.* **1995**, *34*, 1107−1110.

(25) Rodriguez, L.; Oelkers, C.; Aguirrezabalaga, I.; Braña, A. F.; Rohr, J. J.; Méndez, C.; Salas, J. A.; Brana, A. F.; Rohr, J. J.; Mendez, C.; Salas, J. A. Generation of Hybrid Elloramycin Analogs by Combinatorial

Biosynthesis Using Genes from Anthracycline-Type and Macrolide Biosynthetic Pathways. *J. Mol. Microbiol. Biotechnol.* **2000**, *2*, 271−276.
(26) Patallo, E. P.; Blanco, G.; Fischer, C.; Braña, A. F.; Rohr, J.; Méndez, C.; Salas, J. A. Deoxysugar Methylation during Biosynthesis of the Antitumor Polyketide Elloramycin by *Streptomyces olivaceus*: Characterization of Three Methyltransferase Genes. *J. Biol. Chem.* **2001**, *276*, 18765−18774.
(27) Shen, B.; Hutchinson, C. R. Triple Hydroxylation of Tetracenomycin A2 to Tetraenomycin C in *Streptomyces glaucescens*. *J. Biol. Chem.* **1994**, *1326*, 30726−30733.
(28) Thompson, T. B.; Katayama, K.; Watanabe, K.; Hutchinson, C. R.; Rayment, I. Structural and Functional Analysis of Tetracenomycin F2 Cyclase from *Streptomyces glaucescens*: A Type II Polyketide Cyclase. *J. Biol. Chem.* **2004**, *279*, 37956−37963.
(29) Motamedi, H.; Hutchinson, C. R. Cloning and heterologous expression of a gene cluster for the biosynthesis of tetracenomycin C, the anthracycline antitumor antibiotic of *Streptomyces glaucescens*. *Proc. Natl. Acad. Sci. U.S.A.* **1987**, *84*, 4445−4449.
(30) White-Phillip, J.; Thibodeaux, C. J.; Liu, H.Enzymatic Synthesis of TDP-Deoxysugars. *Methods in Enzymology*; Elsevier Inc., 2009; Vol. *459*, pp 521−544.
(31) Lombó, F.; Siems, K.; Braña, A. F.; Méndez, C.; Bindseil, K.; Salas, J. A. Cloning and Insertional Inactivation of *Streptomyces argillaceus* Genes Involved in the Earliest Steps of Biosynthesis of the Sugar Moieties of the Antitumor Polyketide Mithramycin. *J. Bacteriol.* **1997**, *179*, 3354−3357.
(32) Aguirrezabalaga, I.; Olano, C.; Allende, N.; Rodriguez, L.; Braña, A. F.; Méndez, C.; Salas, J. A. Identification and Expression of Genes Involved in Biosynthesis of L-Oleandrose and Its Intermediate L-Olivose in the Oleandomycin Producer *Streptomyces antibioticus*. *Antimicrob. Agents Chemother.* **2000**, *44*, 1266−1275.
(33) Xue, Y.; Zhao, L.; Liu, H. W.; Sherman, D. H. A Gene Cluster for Macrolide Antibiotic Biosynthesis in *Streptomyces venezuelae*: Architecture of Metabolic Diversity. *Proc. Natl. Acad. Sci. U.S.A.* **1998**, *95*, 12111−12116.
(34) Tang, L.; McDaniel, R. Construction of Desosamine Containing Polyketide Libraries Using a Glycosyltransferase with Broad Substrate Specificity. *Chem. Biol.* **2001**, *8*, 547−555.
(35) Knight, T. *Idempotent Vector Design for Standard Assembly of Biobricks Idempotent Vector Design for Standard Assembly of Biobricks*; MIT Articial Intelligence Laboratory, 2003; pp 1−11. http://hdl.handle.net/1721.1/21168.
(36) Shetty, R. P.; Endy, D.; Knight, T. F. Engineering BioBrick Vectors from BioBrick Parts. *J. Biol. Eng.* **2008**, *2*, No. 5.
(37) Elowitz, M. B.; Leibler, S. A Synthetic Oscillatory Network of Transcriptional Regulators. *Nature* **2000**, *403*, 335−338.
(38) Shao, Z.; Rao, G.; Li, C.; Abil, Z.; Luo, Y.; Zhao, H. Refactoring the Silent Spectinabilin Gene Cluster Using a Plug-and-Play Scaffold. *ACS Synth. Biol.* **2013**, *2*, 662−669.
(39) Doumith, M.; Weingarten, P.; Wehmeier, U. F.; Salah-Bey, K.; Benhamou, B.; Capdevila, C.; Michel, J. M.; Piepersberg, W.; Raynal, M. C. Analysis of Genes Involved in 6-Deoxyhexose Biosynthesis and Transfer in *Saccharopolyspora erythraea*. *Mol. Gen. Genet.* **2000**, *264*, 477−485.
(40) MacNeil, D. J.; Gewain, K. M.; Ruby, C. L.; Dezeny, G.; Gibbons, P. H.; MacNeil, T. Analysis of *Streptomyces avermitilis* Genes Required for Avermectin Biosynthesis Utilizing a Novel Integration Vector. *Gene* **1992**, *111*, 61−68.
(41) Gomez-Escribano, J. P.; Bibb, M. J. Engineering *Streptomyces coelicolor* for Heterologous Expression of Secondary Metabolite Gene Clusters. *Microb. Biotechnol.* **2011**, *4*, 207−215.
(42) González, A.; Remsing, L. L.; Lombó, F.; Fernández, M. J.; Prado, L.; Braña, A. F.; Künzel, E.; Rohr, J.; Méndez, C.; Salas, J. A. The MtmVUC Genes of the Mithramycin Gene Cluster in *Streptomyces argillaceus* Are Involved in the Biosynthesis of the Sugar Moieties. *Mol. Gen. Genet.* **2001**, *264*, 827−835.
(43) Remsing, L. L.; Garcia-Bernardo, J.; Gonzalez, A.; Künzel, E.; Rix, U.; Braña, A. F.; Bearden, D. W.; Méndez, C.; Salas, J. A.; Rohr, J. Ketopremithramycins and Ketomithramycins, Four New Aureolic Acid-Type Compounds Obtained upon Inactivation of Two Genes Involved in the Biosynthesis of the Deoxysugar Moieties of the Antitumor Drug Mithramycin by *Streptomyces argillaceus*, Reveal Novel Insights into Post-PKS Tailoring Steps of the Mithramycin Biosynthetic Pathway. *J. Am. Chem. Soc.* **2002**, *124*, 1606−1614.
(44) Wang, G.; Pahari, P.; Kharel, M. K.; Chen, J.; Zhu, H.; Vanlanen, S. G.; Rohr, J. Cooperation of Two Bifunctional Enzymes in the Biosynthesis and Attachment of Deoxysugars of the Antitumor Antibiotic Mithramycin. *Angew. Chem., Int. Ed.* **2012**, *51*, 10638−10642.
(45) Wang, G.; Kharel, M. K.; Pahari, P.; Rohr, J. Investigating Mithramycin Deoxysugar Biosynthesis: Enzymatic Total Synthesis of TDP-D-Olivose. *ChemBioChem* **2011**, *12*, 2568−2571.
(46) Wohlert, S. E.; Blanco, G.; Lombó, F.; Fernández, E.; Braña, A. F.; Reich, S.; Udvarnoki, G.; Méndez, C.; Decker, H.; Frevert, J.; Salas, J. A.; Rohr, J. Novel Hybrid Tetracenomycins through Combinatorial Biosynthesis Using a Glycosyltransferase Encoded by the Elm Genes in Cosmid 16F4 and Which Shows a Broad Sugar Substrate Specificity. *J. Am. Chem. Soc.* **1998**, *120*, 10596−10601.
(47) Menéndez, N.; Nur-e-Alam, M.; Braña, A. F.; Rohr, J.; Salas, J. A.; Méndez, C. Biosynthesis of the Antitumor Chromomycin A3 in *Streptomyces griseus*: Analysis of the Gene Cluster and Rational Design of Novel Chromomycin Analogs. *Chem. Biol.* **2004**, *11*, 21−32.
(48) Menéndez, N.; Nur-E-Alam, M.; Fischer, C.; Braña, A. F.; Salas, J. A.; Rohr, J.; Méndez, C. Deoxysugar Transfer during Chromomycin A3 Biosynthesis in *Streptomyces griseus* Subsp. Griseus: New Derivatives with Antitumor Activity. *Appl. Environ. Microbiol.* **2006**, *72*, 167.
(49) Thuy, T. T. T.; Liou, K.; Oh, T. J.; Kim, D. H.; Nam, D. H.; Yoo, J. C.; Sohng, J. K. Biosynthesis of DTDP-6-Deoxy-β-d-Allose, Biochemical Characterization of DTDP-4-Keto-6-Deoxyglucose Reductase (GerKI) from Streptomyces Sp. KCTC 0041BP. *Glycobiology* **2006**, *17*, 119−126.
(50) Sohng, J.-K.; Kim, H.-J.; Nam, D.-H.; Lim, D.-O.; Han, J. M.; Lee, H.-J.; Yoo, J.-C. Cloning, Expression, and Biological Function of a DTDP-Deoxyglucose Epimerase (GerF) Gene from Streptomyces Sp. GERI-155. *Biotechnol. Lett.* **2004**, *26*, 185−191.
(51) Borisova, S. A.; Zhao, L.; Sherman, D. H.; Liu, H. W. Biosynthesis of desosamine: construction of a new macrolide carrying a genetically designed sugar moiety. *Org. Lett.* **1999**, *1*, 133−136.
(52) Fischer, C.; Lipata, F.; Rohr, J. The Complete Gene Cluster of the Antitumor Agent Gilvocarcin V and Its Implication for the Biosynthesis of the Gilvocarcins. *J. Am. Chem. Soc.* **2003**, *125*, 7818−7819.
(53) Takahashi, K.; Yoshida, M.; Tomita, F.; Shirahata, K. Gilvocarcins, new antitumor antibiotics. 2. Structural elucidation. *J. Antibiot.* **1981**, *34*, 271−275.
(54) Liu, T.; Fischer, C.; Beninga, C.; Rohr, J. Oxidative Rearrangement Processes in the Biosynthesis of Gilvocarcin V. *J. Am. Chem. Soc.* **2004**, *126*, 12262−12263.
(55) Kharel, M. K.; Pahari, P.; Lian, H.; Rohr, J. GilR, an Unusual Lactone-Forming Enzyme Involved in Gilvocarcin Biosynthesis. *ChemBioChem* **2009**, *10*, 1305−1308.
(56) Pahari, P.; Kharel, M. K.; Shepherd, M. D.; van Lanen, S. G.; Rohr, J. Enzymatic Total Synthesis of Defucogilvocarcin M and Its Implications for Gilvocarcin Biosynthesis. *Angew. Chem., Int. Ed.* **2012**, *51*, 1216−1220.
(57) Tibrewal, N.; Pahari, P.; Wang, G.; Kharel, M. K.; Morris, C.; Downey, T.; Hou, Y.; Bugni, T. S.; Rohr, J. Baeyer-Villiger C-C Bond Cleavage Reaction in Gilvocarcin and Jadomycin Biosynthesis. *J. Am. Chem. Soc.* **2012**, *134*, 18181−18184.
(58) Kharel, M. K.; Pahari, P.; Lian, H.; Rohr, J. Enzymatic Total Synthesis of Rabelomycin, an Angucycline Group Antibiotic. *Org. Lett.* **2010**, *12*, 2814−2817.
(59) Shepherd, M. D.; Kharel, M. K.; Zhu, L. L.; van Lanen, S. G.; Rohr, J. Delineating the Earliest Steps of Gilvocarcin Biosynthesis: Role of GilP and GilQ in Starter Unit Specificity. *Org. Biomol. Chem.* **2010**, *8*, 3851−3856.
(60) Kharel, M. K.; Zhu, L.; Liu, T.; Rohr, J. Multi-Oxygenase Complexes of the Gilvocarcin and Jadomycin Biosyntheses. *J. Am. Chem. Soc.* **2007**, *129*, 3780−3781.

https://doi.org/10.1021/acsomega.3c02460
ACS Omega 2023, 8, 21237−21253

(61) Tibrewal, N.; Downey, T. E.; van Lanen, S. G.; Ul Sharif, E.; O'Doherty, G. A.; Rohr, J. Roles of the Synergistic Reductive O-Methyltransferase GilM and of O-Methyltransferase GilMT in the Gilvocarcin Biosynthetic Pathway. *J. Am. Chem. Soc.* **2012**, *134*, 12402−12405.
(62) Noinaj, N.; Bosserman, M. A.; Schickli, M. A.; Piszczek, G.; Kharel, M. K.; Pahari, P.; Buchanan, S. K.; Rohr, J. The Crystal Structure and Mechanism of an Unusual Oxidoreductase, GilR, Involved in Gilvocarcin V Biosynthesis. *J. Biol. Chem.* **2011**, *286*, 23533−23543.
(63) Liu, T.; Kharel, M. K.; Zhu, L.; Bright, S. A.; Mattingly, C.; Adams, V. R.; Rohr, J. Inactivation of the Ketoreductase GilU Gene of the Gilvocarcin Biosynthetic Gene Cluster Yields New Analogues with Partly Improved Biological Activity. *ChemBioChem* **2009**, *10*, 278−286.
(64) Kharel, M. K.; Nybo, S. E.; Shepherd, M. D.; Rohr, J. Cloning and characterization of the ravidomycin and chrysomycin biosynthetic gene clusters. *ChemBioChem* **2010**, *11*, 523−532.
(65) Liu, T.; Kharel, M. K.; Fischer, C.; McCormick, A.; Rohr, J. Inactivation of GilGT, Encoding a *C*-Glycosyltransferase, and GilOIII, Encoding a P450 Enzyme, Allows the Details of the Late Biosynthetic Pathway to Gilvocarcin V to Be Delineated. *ChemBioChem* **2006**, *7*, 1070−1077.
(66) Shepherd, M. D.; Liu, T.; Méndez, C.; Salas, J. A.; Rohr, J. Engineered Biosynthesis of Gilvocarcin Analogues with Altered Deoxyhexopyranose Moieties. *Appl. Environ. Microbiol.* **2011**, *77*, 435−441.
(67) Chen, J. M.; Shepherd, M. D.; Horn, J.; Leggas, M.; Rohr, J. Enzymatic Methylation and Structure-Activity-Relationship Studies on Polycarcin V, a Gilvocarcin-Type Antitumor Agent. *ChemBioChem* **2014**, *15*, 2729−2735.
(68) Ma, R.; Cheng, S.; Sun, J.; Zhu, W.; Fu, P. Antibacterial Gilvocarcin-Type Aryl-C-Glycosides from a Soil-Derived *Streptomyces* Species. *J. Nat. Prod.* **2022**, *85*, 2282−2289.
(69) Kharel, M. K.; Rohr, J. Delineation of Gilvocarcin, Jadomycin, and Landomycin Pathways through Combinatorial Biosynthetic Enzymology. *Curr. Opin. Chem. Biol.* **2012**, *16*, 150−161.
(70) Yan, Y.; Yang, J.; Wang, L.; Xu, D.; Yu, Z.; Guo, X.; Horsman, G. P.; Lin, S.; Tao, M.; Huang, S. X. Biosynthetic access to the rare antiarose sugar via an unusual reductase-epimerase. *Chem. Sci.* **2020**, *11*, 3959−3964.
(71) Fiedler, H. P.; Rohr, J.; Zeeck, A. Elloramycins B, C, D, E and F: Minor Congeners of the Elloramycin Producer *Streptomyces olivaceus*. *J. Antibiot.* **1986**, *39*, 856−859.
(72) Williams, G. J.; Zhang, C.; Thorson, J. S. Expanding the Promiscuity of a Natural-Product Glycosyltransferase by Directed Evolution. *Nat. Chem. Biol.* **2007**, *3*, 657−662.
(73) Williams, G. J.; Goff, R. D.; Zhang, C.; Thorson, J. S. Optimizing Glycosyltransferase Specificity via "Hot Spot" Saturation Mutagenesis Presents a Catalyst for Novobiocin Glycorandomization. *Chem. Biol.* **2008**, *15*, 393−401.
(74) Gantt, R. W.; Peltier-Pain, P.; Singh, S.; Zhou, M.; Thorson, J. S. Broadening the Scope of Glycosyltransferase-Catalyzed Sugar Nucleotide Synthesis. *Proc. Natl. Acad. Sci. U.S.A.* **2013**, *110*, 7648−7653.
(75) Borisova, S. A.; Liu, H.-W. W. Characterization of Glycosyltransferase DesVII and Its Auxiliary Partner Protein DesVIII in the Methymycin/Pikromycin Biosynthetic Pathway. *Biochemistry* **2010**, *49*, 8071−8084.
(76) Kao, C. L.; Borisova, S. A.; Kim, H. J.; Liu, H. W. Linear Aglycones Are the Substrates for Glycosyltransferase DesVII in Methymycin Biosynthesis: Analysis and Implications. *J. Am. Chem. Soc.* **2006**, *128*, 5606−5607.
(77) Borisova, S. A.; Zhao, L.; Melançon, C. E.; Kao, C.-L.; Liu, H. W. Characterization of the Glycosyltransferase Activity of DesVII: Analysis of and Implications for the Biosynthesis of Macrolide Antibiotics. *J. Am. Chem. Soc.* **2004**, *126*, 6534−6535.
(78) Kieser, T.; Bibb, M. J.; Buttner, M. J.; Chater, K. F.; Hopwood, D. A. *Practical Streptomyces Genetics*; John Innes Foundation: Norwich, 2000; p 529.
(79) Sambrook, J.; Russell, D. W. *Molecular Cloning: A Laboratory Manual*; Cold Spring Harbor Laboratory Press: NY, 2001; p 999.
(80) Shaaban, K. A.; Wang, X.; Elshahawi, S. I.; Ponomareva, L. V.; Sunkara, M.; Copley, G. C.; Hower, J. C.; Morris, A. J.; Kharel, M. K.; Thorson, J. S.; Herbimycins, D.-F. Ansamycin Analogues from *Streptomyces* sp. RM-7-15. *J. Nat. Prod.* **2013**, *76*, 1619−1626.
(81) Wang, X.; Shaaban, K. A.; Elshahawi, S. I.; Ponomareva, L. V.; Sunkara, M.; Zhang, Y.; Copley, G. C.; Hower, J. C.; Morris, A. J.; Kharel, M. K.; Thorson, J. S. Frenolicins C-G, Pyranonaphthoquinones from *Streptomyces* sp. RM-4-15. *J. Nat. Prod.* **2013**, *76*, 1441−1447.
(82) Shaaban, K. A.; Elshahawi, S. I.; Wang, X.; Horn, J.; Kharel, M. K.; Leggas, M.; Thorson, J. S. Cytotoxic Indolocarbazoles from *Actinomadura melliaura* ATCC 39691. *J. Nat. Prod.* **2015**, *78*, 1723−1729.
(83) Savi, D. C.; Shaaban, K. A.; Wilke, F. M.; Gos, R.; Ponomareva, L. V.; Thorson, J. S.; Glienke, C.; Rohr, J. *Phaeophleospora vochysiae* Savi & Glienke Sp. Nov. Isolated from *Vochysia divergens* Found in the Pantanal, Brazil, Produces Bioactive Secondary Metabolites. *Sci. Rep.* **2018**, *8*, No. 3122.
(84) Hailu, W.; Helmy, Y. A.; Carney-Knisely, G.; Kauffman, M.; Fraga, D.; Rajashekara, G. Prevalence and Antimicrobial Resistance Profiles of Foodborne Pathogens Isolated from Dairy Cattle and Poultry Manure Amended Farms in Northeastern Ohio, the United States. *Antibiotics* **2021**, *10*, No. 1450.
(85) Helmy, Y. A.; Deblais, L.; Kassem, I. I.; Kathayat, D.; Rajashekara, G. Novel small molecule modulators of quorum sensing in avian pathogenic *Escherichia coli* (APEC). *Virulence* **2018**, *9*, 1640−1657.
(86) Deblais, L.; Helmy, Y. A.; Kumar, A.; Antwi, J.; Kathayat, D.; Acuna, U. M.; Huang, H. C.; de Blanco, E. C.; Fuchs, J. R.; Rajashekara, G. Novel narrow spectrum benzyl thiophene sulfonamide derivatives to control Campylobacter. *J. Antibiot.* **2019**, *72*, 555−565.
(87) Deblais, L.; Helmy, Y. A.; Kathayat, D.; Huang, H. C.; Miller, S. A.; Rajashekara, G. Novel Imidazole and Methoxybenzylamine Growth Inhibitors Affecting Salmonella Cell Envelope Integrity and its Persistence in Chickens. *Sci. Rep.* **2018**, *8*, No. 13381.

https://doi.org/10.1021/acsomega.3c02460
ACS Omega 2023, 8, 21237−21253